

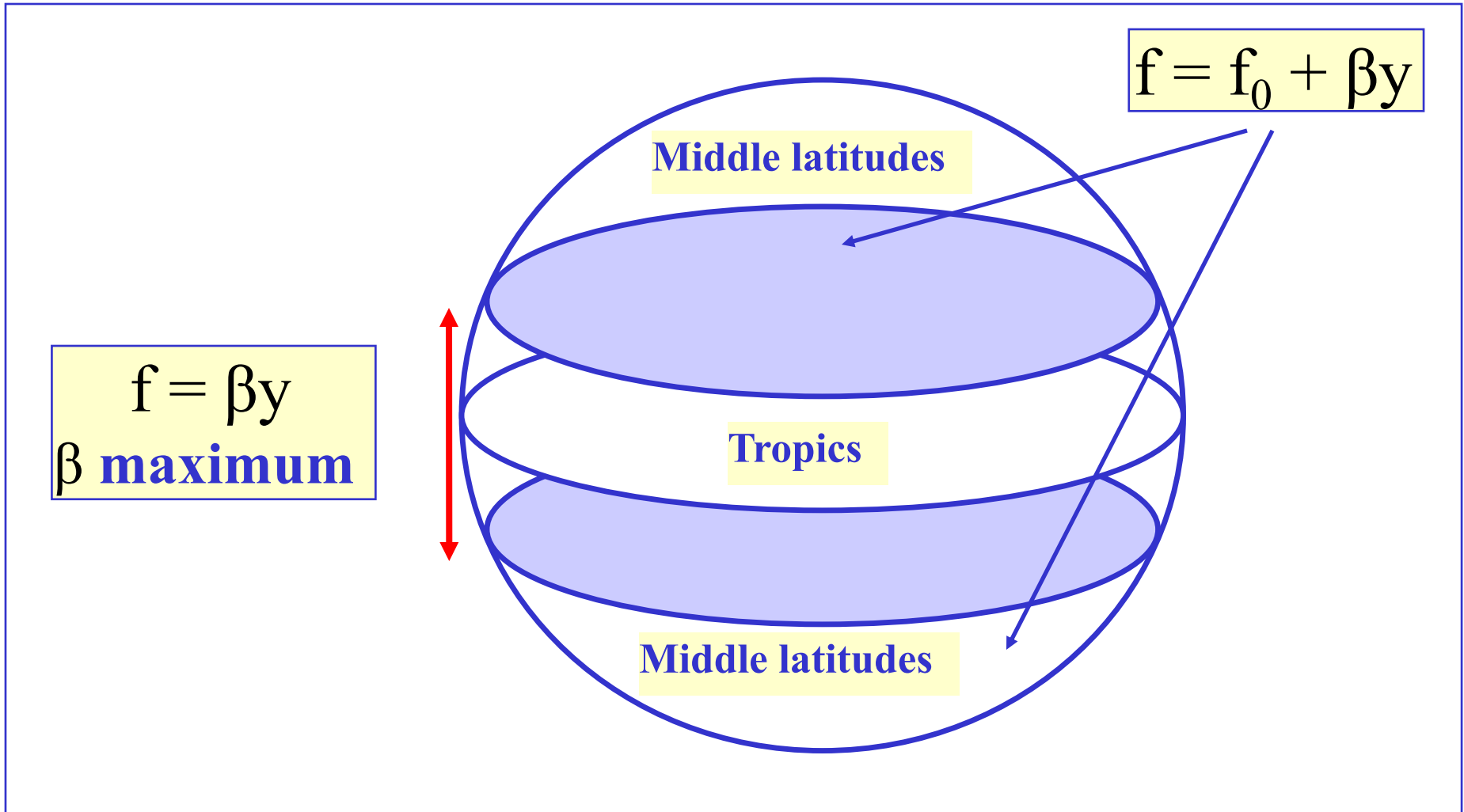
MR3252: Tropical Meteorology

Equatorial Wave Theory

Main Topics:

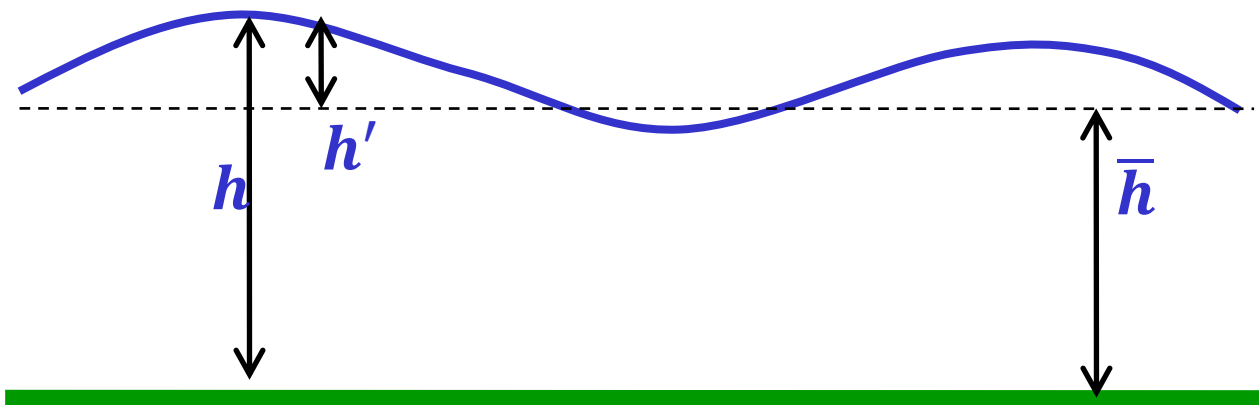
- Matsuno theory for free equatorial waves
- Dispersion diagrams
- Wave tracking

Tropics versus Middle Latitudes



Shallow Water Equations on an Equatorial beta-plane

- At the equator $f_0=0$, and β is a maximum
- Use shallow water equations as a starting point to understand wave motions in the tropics



$$\frac{\partial u}{\partial t} - \beta y v + g \frac{\partial h'}{\partial x} = 0$$

$$\frac{\partial v}{\partial t} + \beta y u + g \frac{\partial h'}{\partial y} = 0$$

$$\frac{\partial h'}{\partial t} + \frac{\partial(\bar{h}u)}{\partial x} + \frac{\partial(\bar{h}v)}{\partial y} = 0$$

Beta-plane approximation: $f = \beta y$

- Linearize about a basic resting mean state to find wave perturbations.

$$\frac{\partial u}{\partial t} - \beta y v + g \frac{\partial h'}{\partial x} = 0$$


$$\frac{\partial v}{\partial t} + \beta y u + g \frac{\partial h'}{\partial y} = 0$$

$$\frac{\partial h'}{\partial t} + \frac{\partial(\bar{h}u)}{\partial x} + \frac{\partial(\bar{h}v)}{\partial y} = 0$$

$$u(x, y, t) = \bar{u} + u'(x, y, t)$$

$$v(x, y, t) = \bar{v} + v'(x, y, t)$$

Resting state: $\bar{u}=0, \bar{v}=0$

$\phi = gh$


$$\frac{\partial u'}{\partial t} - \beta y v' + \frac{\partial \phi'}{\partial x} = 0$$

$$\frac{\partial v'}{\partial t} + \beta y u' + \frac{\partial \phi'}{\partial y} = 0$$

$$\frac{\partial \phi'}{\partial t} + c^2 \left(\frac{\partial u'}{\partial x} + \frac{\partial v'}{\partial y} \right) = 0$$

Gravity wave phase speed

$$c = \sqrt{g\bar{h}}$$

Assume wave-like solutions in the zonal direction and in time, and arbitrary structure in the meridional direction

$$u'(x, y, t) = \hat{u}(y)e^{i(kx-\omega t)}$$

$$v'(x, y, t) = \hat{v}(y)e^{i(kx-\omega t)}$$

$$\phi'(x, y, t) = \hat{\phi}(y)e^{i(kx-\omega t)}$$

Caret denotes variable in y-direction only

Substitute into previous equation set, and eliminate u' and ϕ' :

$$\frac{\partial^2 \hat{v}}{\partial y^2} + \left[\left(\frac{\omega^2}{c^2} - k^2 + \frac{k}{\omega} \beta \right) - \frac{\beta^2 y^2}{c^2} \right] \hat{v} = 0$$

Before moving forward, scale length and time so that the velocity scale is simply c ($L/T = c$). Not required; mainly for convenience of derivation:

$$L \equiv \sqrt{\frac{c}{\beta}} \quad \text{and} \quad T \equiv \frac{1}{\sqrt{c\beta}} \quad \longrightarrow \quad \frac{\partial^2 \hat{v}}{\partial y^2} + \left[\left(\omega^2 - k^2 + \frac{k}{\omega} \right) - y^2 \right] \hat{v} = 0$$

$$\frac{\partial^2 \hat{v}}{\partial y^2} + \left[\left(\omega^2 - k^2 + \frac{k}{\omega} \right) - y^2 \right] \hat{v} = 0$$

We can assert that v goes to zero as y goes to large values. This is our boundary condition. Then we are just left with Schrödinger's equation!

Solutions that are bounded as y approaches infinity are possible only if

$$\left(\omega^2 - k^2 + \frac{k}{\omega} \right) = 2n + 1 \quad \longleftarrow \quad \text{Dispersion relation}$$

Solutions have the meridional structure of parabolic cylinder functions.

$$v'(x, y, t) = H_n(y) C e^{-\frac{y^2}{2}} e^{i(kx - \omega t)}$$

Family of Hermite polynomials: $H_n(y) = (-1)^n e^{y^2} \frac{d^n}{dy^n} (e^{-y^2})$

$$H_0(y) = 1 \quad H_1(y) = 2y \quad H_2(y) = 4y^2 - 2 \quad \text{etc...}$$

Given this dispersion relation, we can solve given some specific cases:

$$\left(\omega^2 - k^2 + \frac{k}{\omega}\right) = 2n + 1$$

First, let's take the limit for small ω ($\omega^2 \ll \omega$):

$$\omega = \frac{k}{k^2 + 2n + 1}$$

If we had not scaled, we would get:

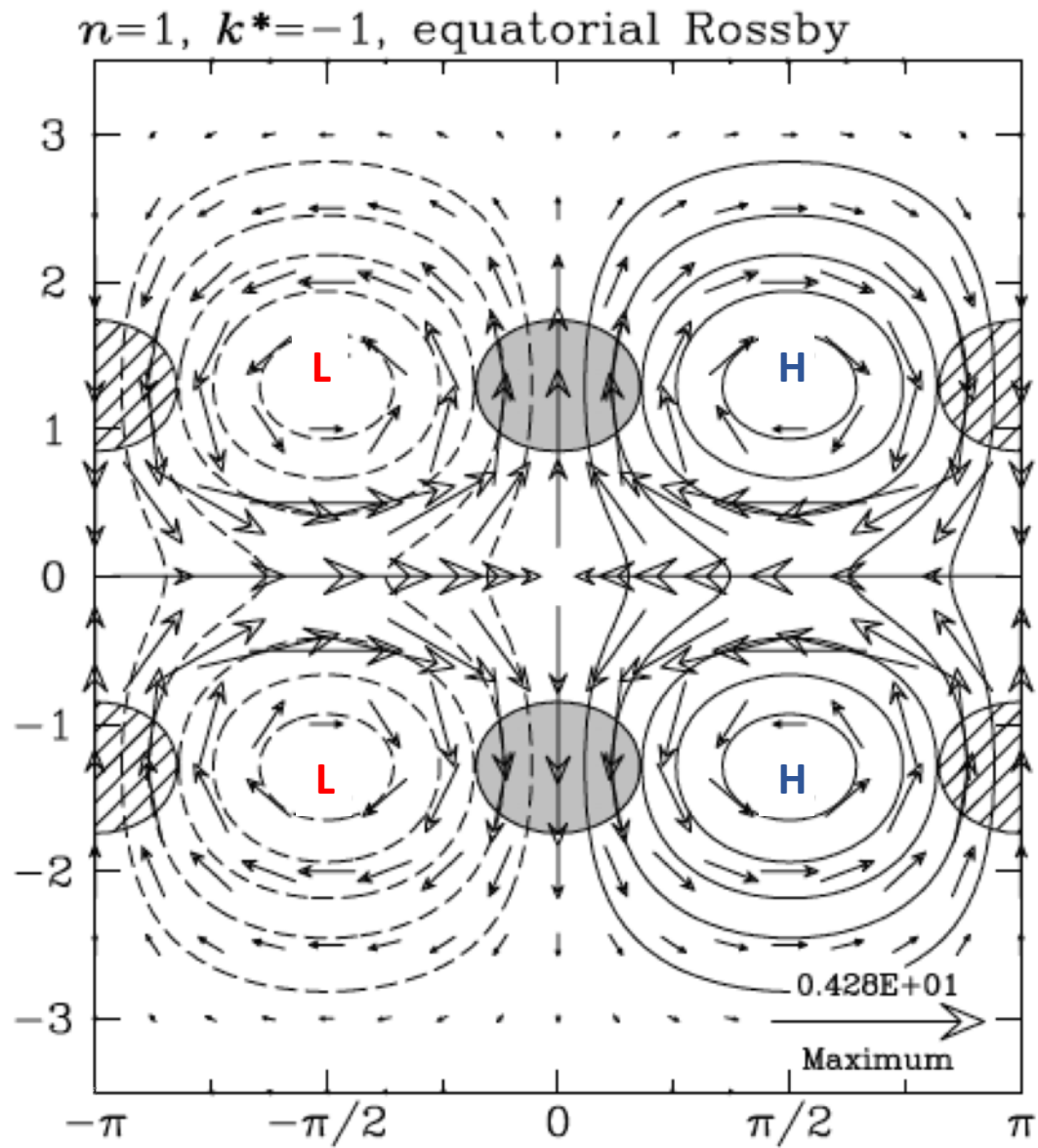
$$\omega = \frac{-\beta k}{k^2 + (2n + 1)\beta/c}$$

This is an **equatorial Rossby wave**.

This is a **dispersive** wave, meaning that phase speed and group velocity are not the same.

$$c_p = \frac{\omega}{k} \quad c_g = \frac{\partial \omega}{\partial k}$$

Equatorial Rossby wave



$$\left(\omega^2 - k^2 + \frac{k}{\omega}\right) = 2n + 1$$

Next, let's take the limit for large ω ($\omega^2 \gg \omega$):

$$\omega = \sqrt{k^2 + 2n + 1}$$

If we had not scaled, we would get:

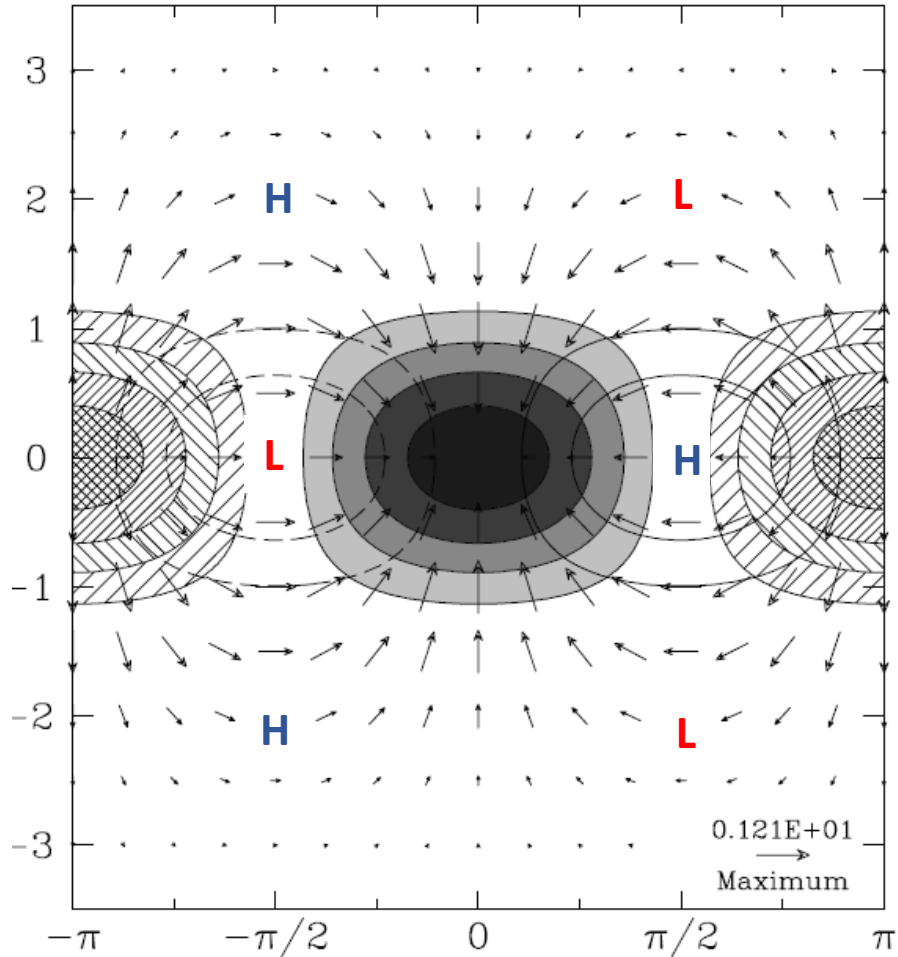
$$\omega^2 = (2n + 1)\beta c + k^2 c^2$$

These represent a family of **inertio-gravity waves**.

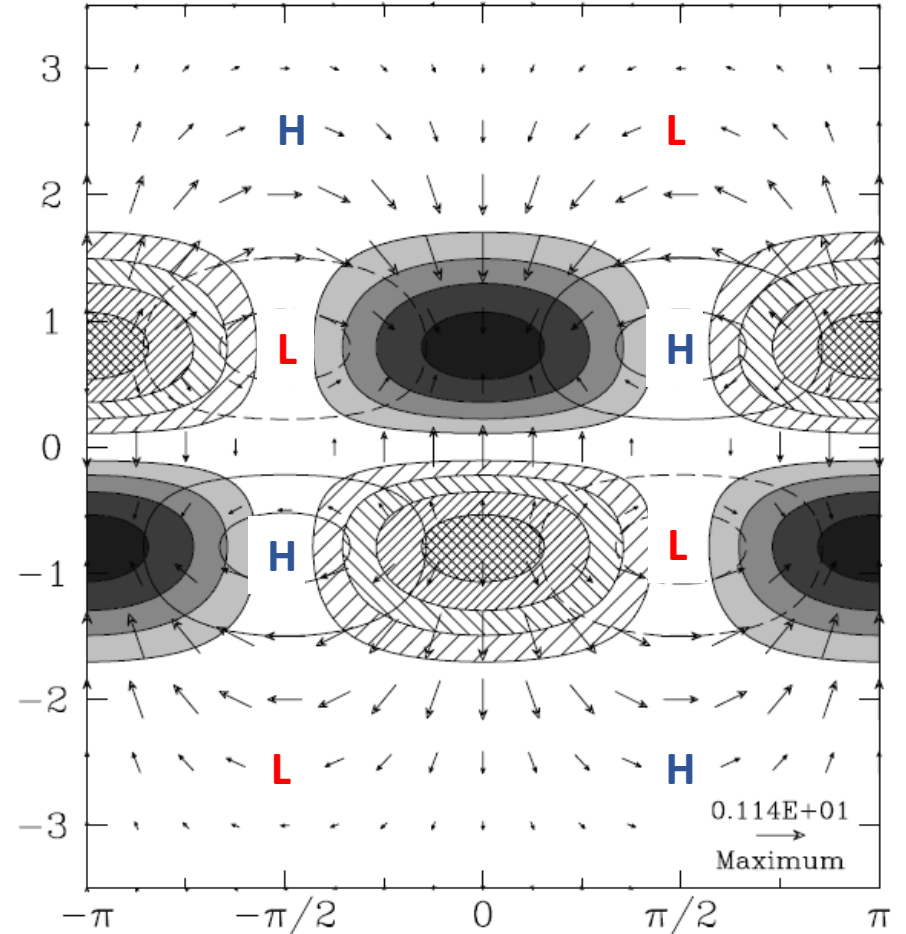
- Equatorially-trapped gravity or Poincaré waves
- Small wavenumbers behave like inertio-gravity waves
- Large wavenumbers behave like pure gravity waves

Westward propagating inertio-gravity wave

$n=1, k^*=-1$, westward inertio-gravity



$n=2, k^*=-1$, westward inertio-gravity



$$\left(\omega^2 - k^2 + \frac{k}{\omega}\right) = 2n + 1$$

Now, let's take the special case of $n = 0$:

$$\left(\omega^2 - k^2 + \frac{k}{\omega}\right) = 1$$

This simpler relation can be factored:

$$(\omega - k)(\omega^2 + \omega k - 1) = 0$$

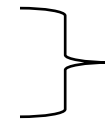
Our new equation has three obvious roots:

~~$$\omega = k$$~~

$$\omega = -\frac{k}{2} \pm \sqrt{\frac{k^2}{4} + 1}$$

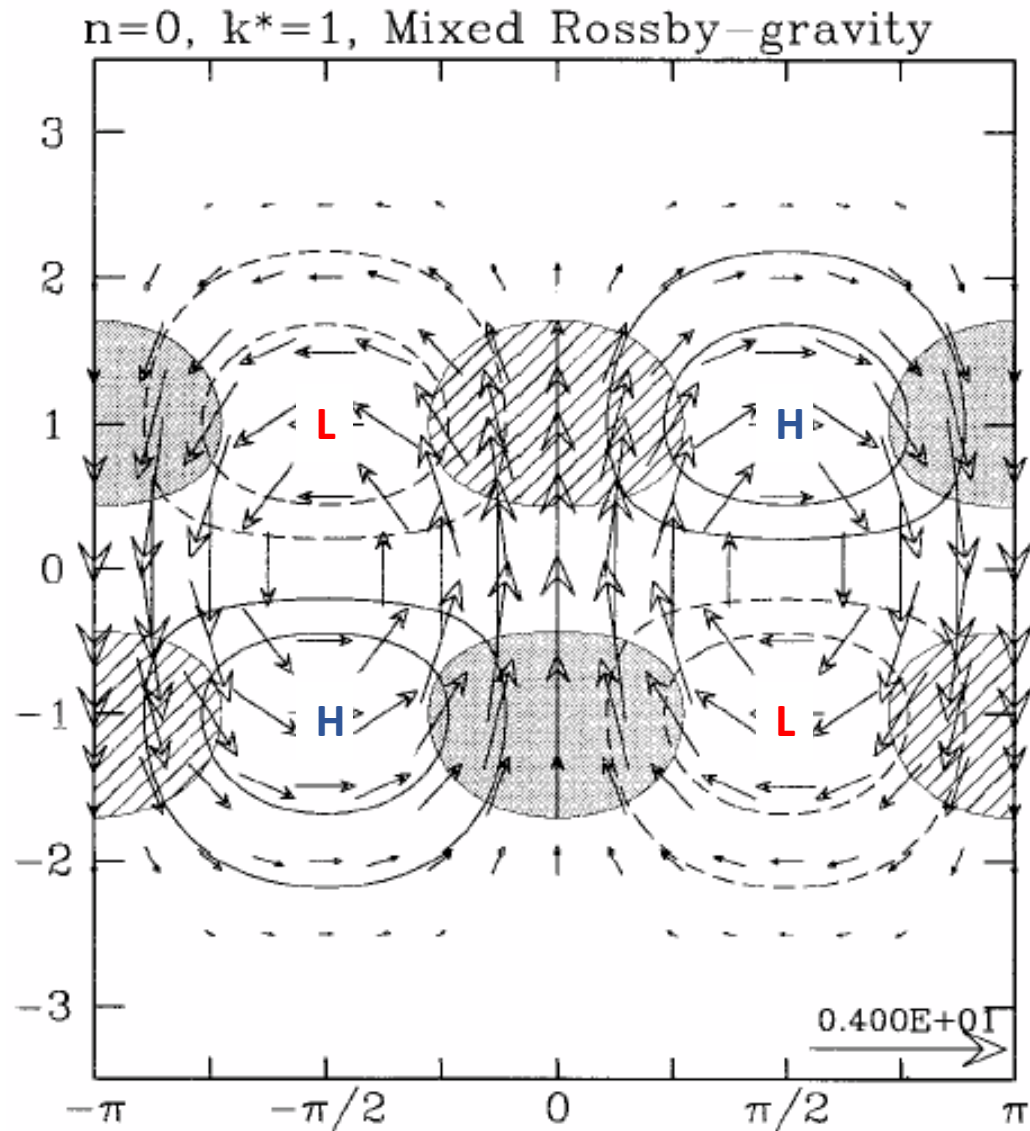
$$\omega = -\frac{1}{2}kc \pm \sqrt{\frac{k^2 c^2}{4} + c\beta}$$

- Positive root is an eastward propagating inertio-gravity wave
- For small k , negative root is a westward propagating inertia-gravity wave
- For large k , negative root is a westward propagating Rossby wave
- Phase velocity can be eastward or westward
- Group velocity is always eastward

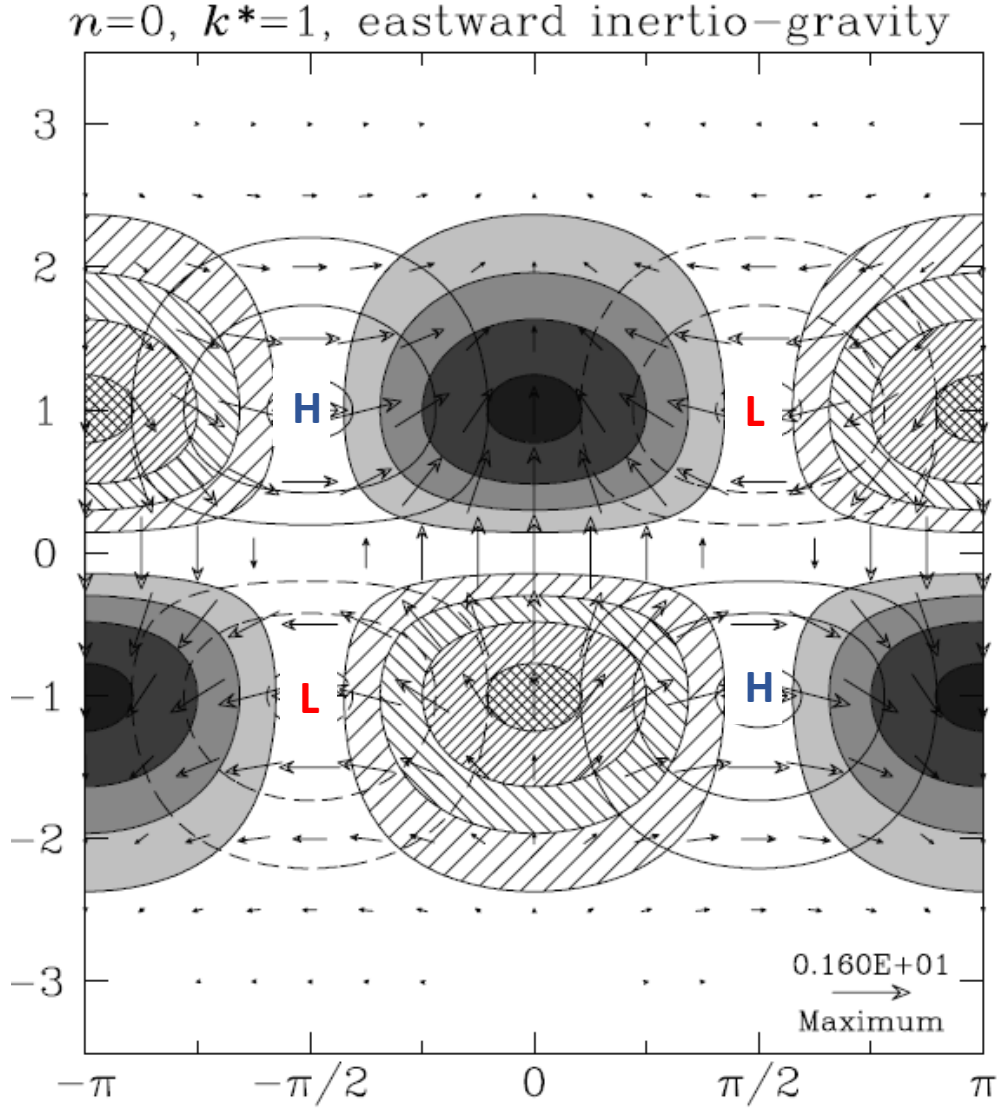


**Mixed
Rossby-
gravity
wave**

Mixed Rossby-gravity (Yanai) wave



$n=0$ Eastward-propagating inertio-gravity wave



There is one additional special case that follows from taking $v' = 0$ and bypassing our dispersion relation. In this case, our equations of motion simplify to

$$\begin{array}{ccc}
 \frac{\partial u'}{\partial t} - \beta y v' + \frac{\partial \phi'}{\partial x} = 0 & & \frac{\partial u'}{\partial t} + \frac{\partial \phi'}{\partial x} = 0 \\
 \frac{\partial v'}{\partial t} + \beta y u' + \frac{\partial \phi'}{\partial y} = 0 & \xrightarrow{v' = 0} & \beta y u' + \frac{\partial \phi'}{\partial y} = 0 \\
 \frac{\partial \phi'}{\partial t} + c^2 \left(\frac{\partial u'}{\partial x} + \frac{\partial v'}{\partial y} \right) = 0 & & \frac{\partial \phi'}{\partial t} + c^2 \left(\frac{\partial u'}{\partial x} \right) = 0
 \end{array}$$

Substitute in assumed solution:

$$\begin{aligned}
 u'(x, y, t) &= \hat{u}(y) e^{i(kx - \omega t)} \\
 \phi'(x, y, t) &= \hat{\phi}(y) e^{i(kx - \omega t)}
 \end{aligned}$$

Solutions only when $\omega = \pm kc$

Reject $\omega = -kc$ because it does not yield solution that decays with latitude.

Solution is an **equatorial Kelvin wave**.

Final solution:

$$u'(x, y, t) = C e^{-\frac{\beta y^2}{2c}} e^{i(kx - \omega t)}$$

$$\phi'(x, y, t) = C e^{-\frac{\beta y^2}{2c}} e^{i(kx - \omega t)}$$

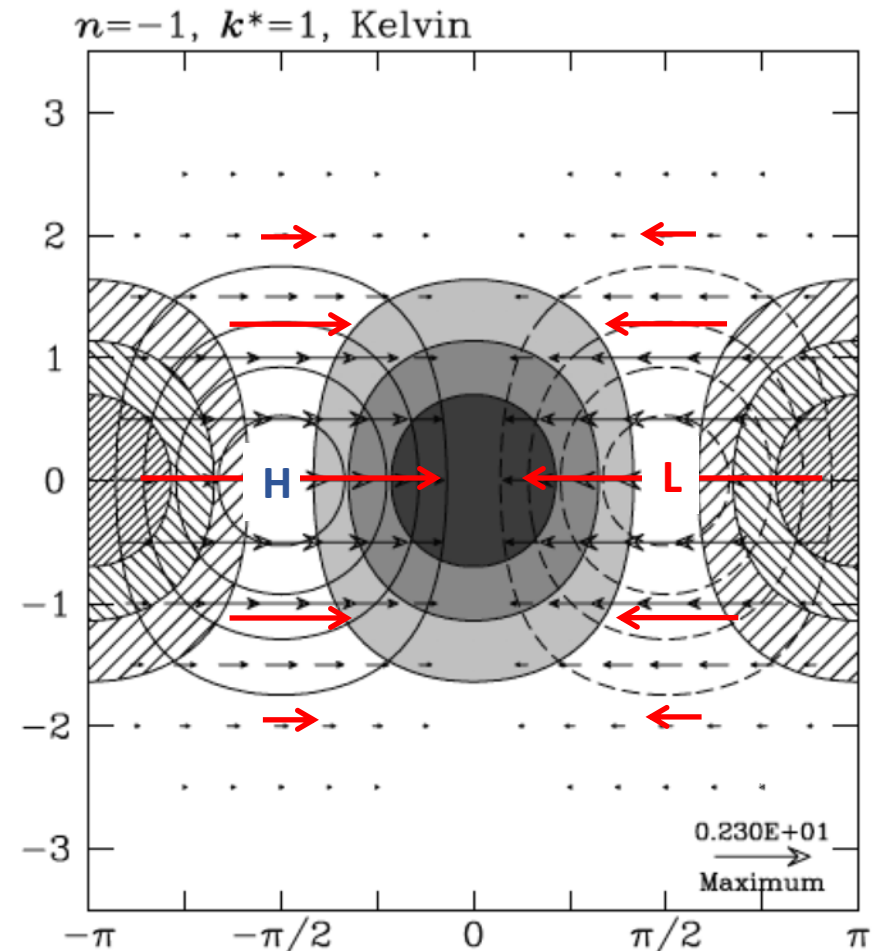
$$v'(x, y, t) = 0$$

$$\omega = kc$$

Phase speed:

$$c = \sqrt{g\bar{h}}$$

- Nondispersive
- Eastward propagating wave
- Trapped in equatorial waveguide by Coriolis forces
- Essentially a Poincaré wave, but with $f = 0$ at equator.
- Satisfies general dispersion relation for $n = -1$.



Dispersion Diagram

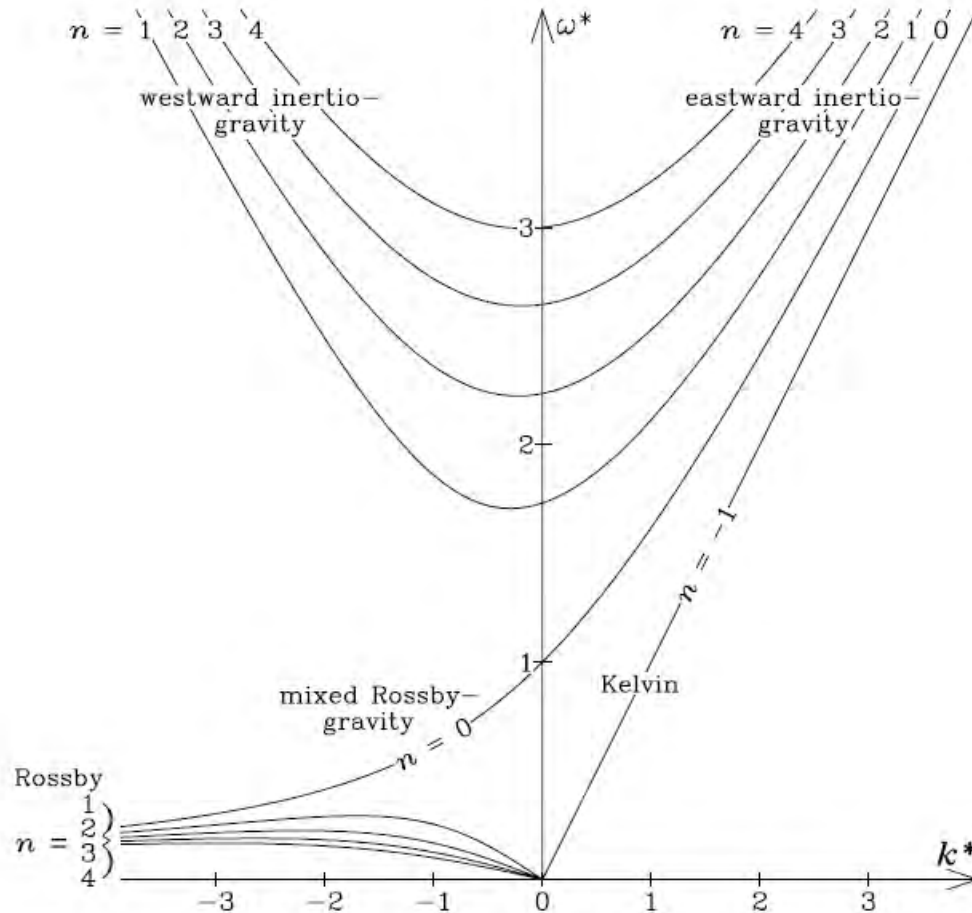
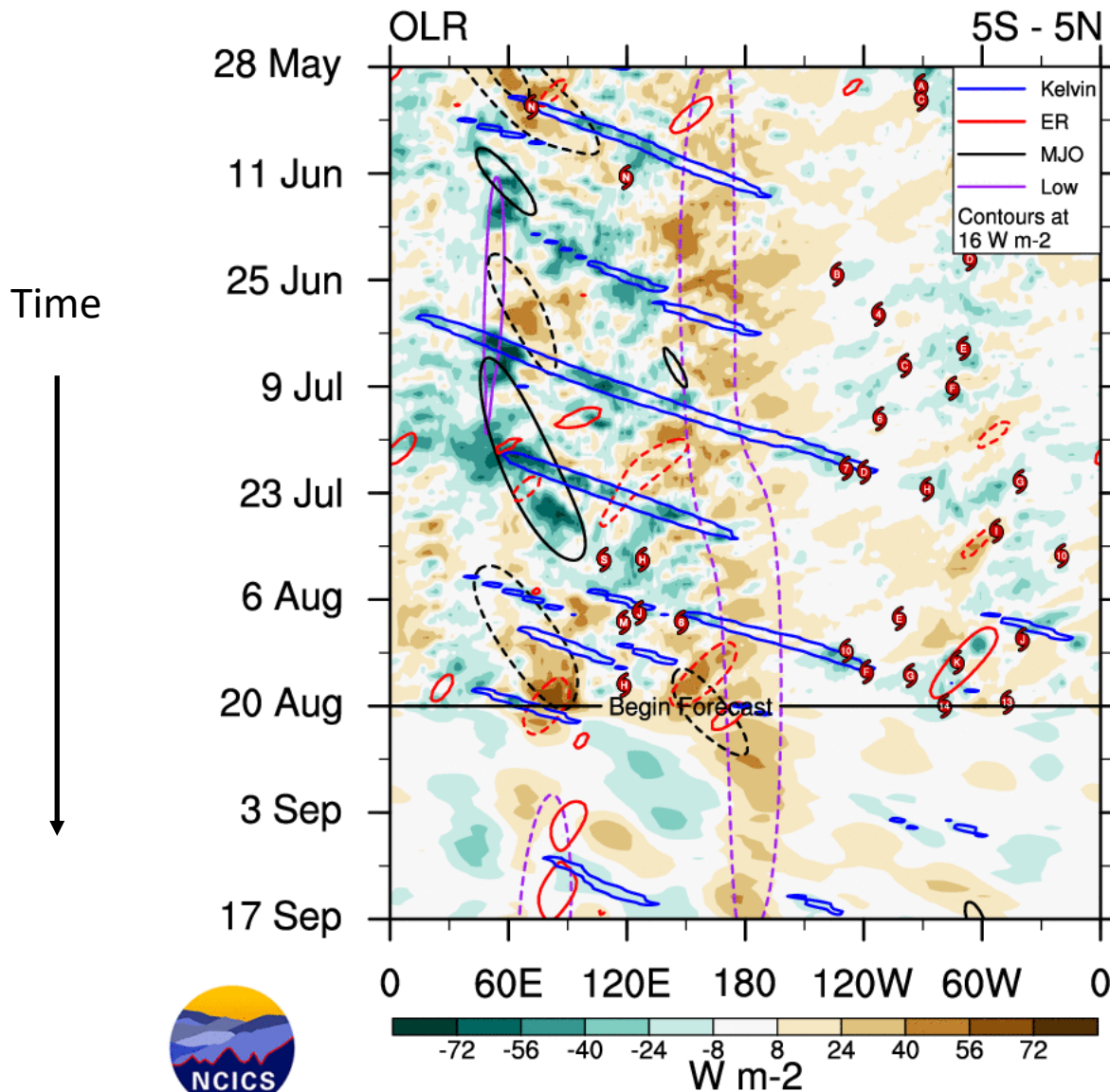


Figure 2. Dispersion curves for equatorial waves (up to $n = 4$) as a function of the nondimensional frequency, ω^* , and nondimensional zonal wave number, k^* , where $\omega^* \equiv \omega/(\beta\sqrt{gh_e})^{1/2}$, and $k^* \equiv k(\sqrt{gh_e}/\beta)^{1/2}$. For all but the Kelvin wave, these dispersion curves are solutions of equation (6). Westward propagating waves (relative to the zero basic state) appear on the left, and eastward propagating waves appear on the right. For consistency with equation (6), the Kelvin wave solution is labeled as $n = -1$.

Outgoing Longwave Radiation Anomaly



Method for real-time tracking of equatorial waves developed by Wheeler and Weickmann (2001).

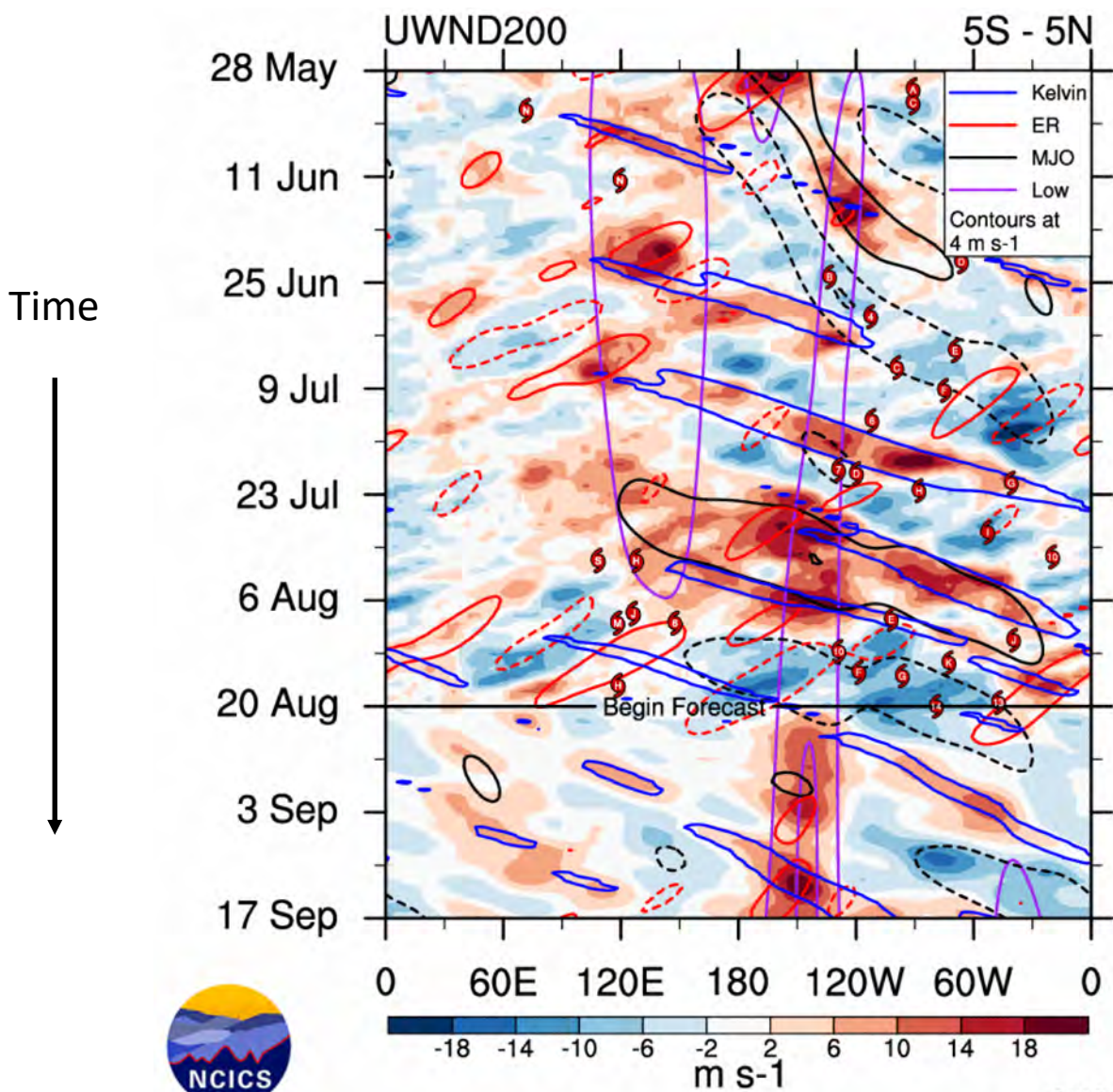


ncics.org/mjo

Fri 2020-08-21 1510 UTC

Carl Schreck
carl_schreck@ncsu.edu

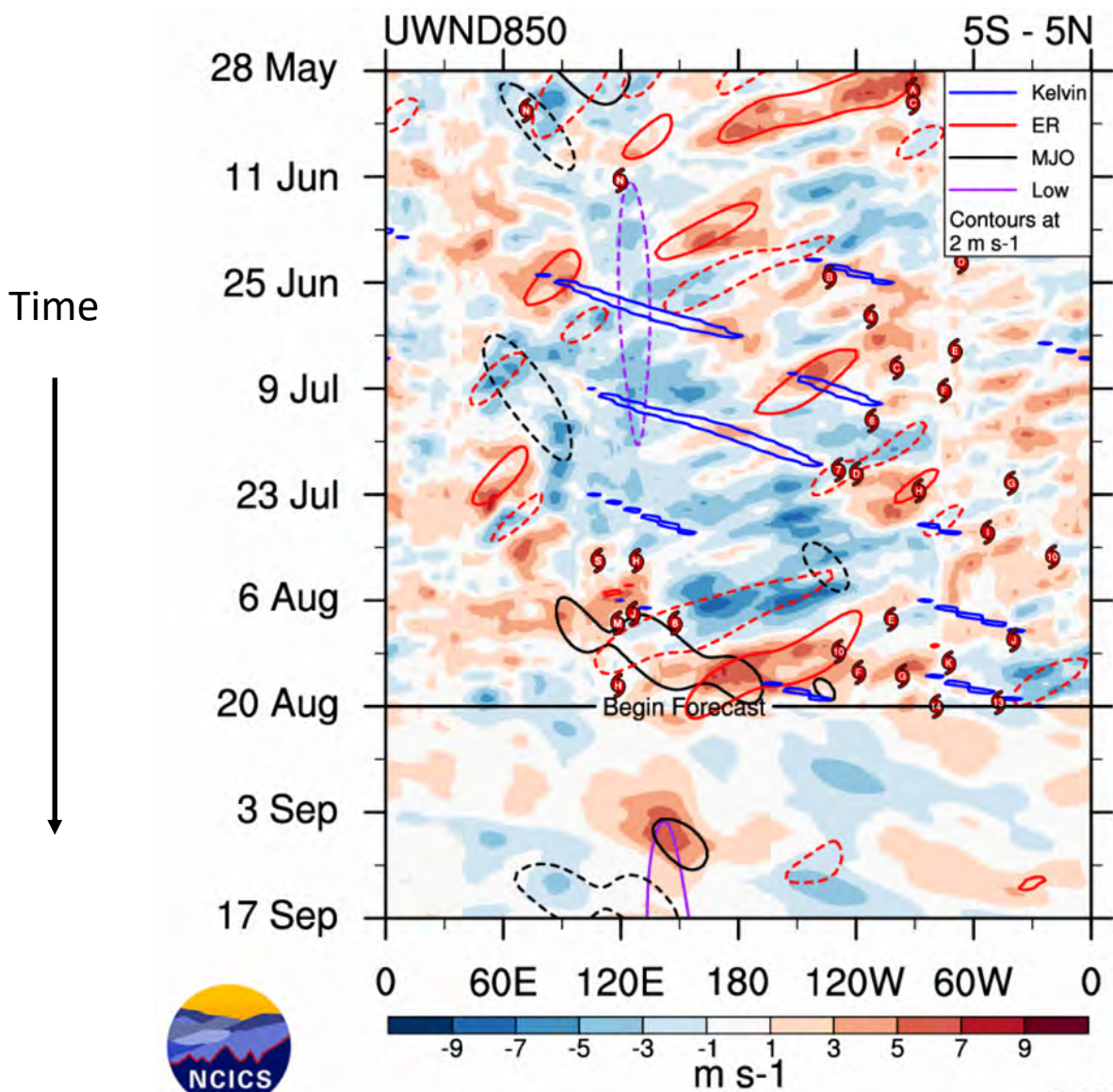
200 hPa Zonal Wind Anomaly



Fri 2020-08-21 1100 UTC

Carl Schreck
carl_schreck@ncsu.edu

850 hPa Zonal Wind Anomaly

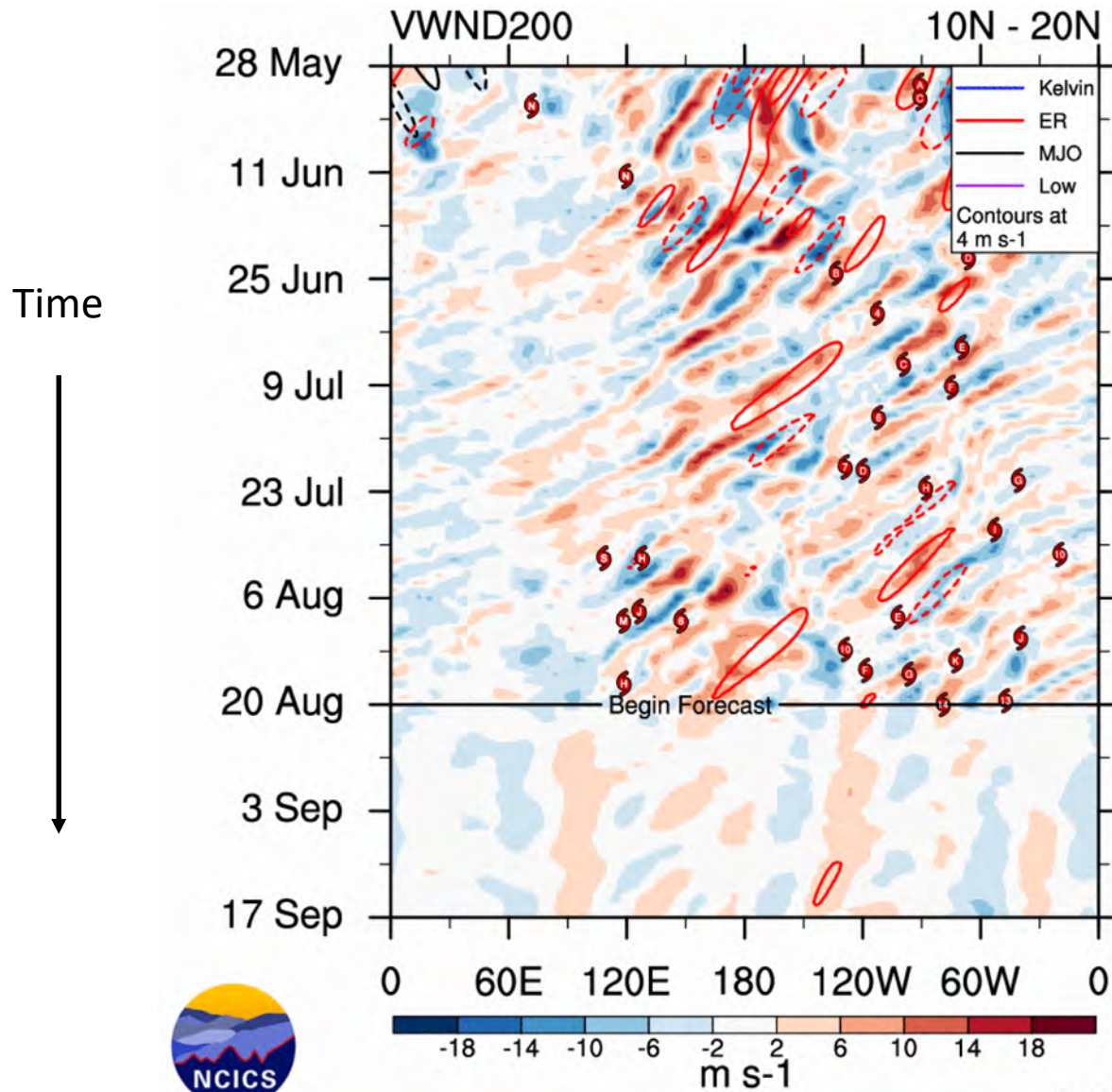


ncics.org/mjo

Fri 2020-08-21 1043 UTC

Carl Schreck
carl_schreck@ncsu.edu

200 hPa Meridional Wind Anomaly (Off-Equator)



ncics.org/mjo

Fri 2020-08-21 1048 UTC

Carl Schreck
carl_schreck@ncsu.edu

MR3252: Tropical Meteorology

Vertical Structure of Coupled Equatorial Waves

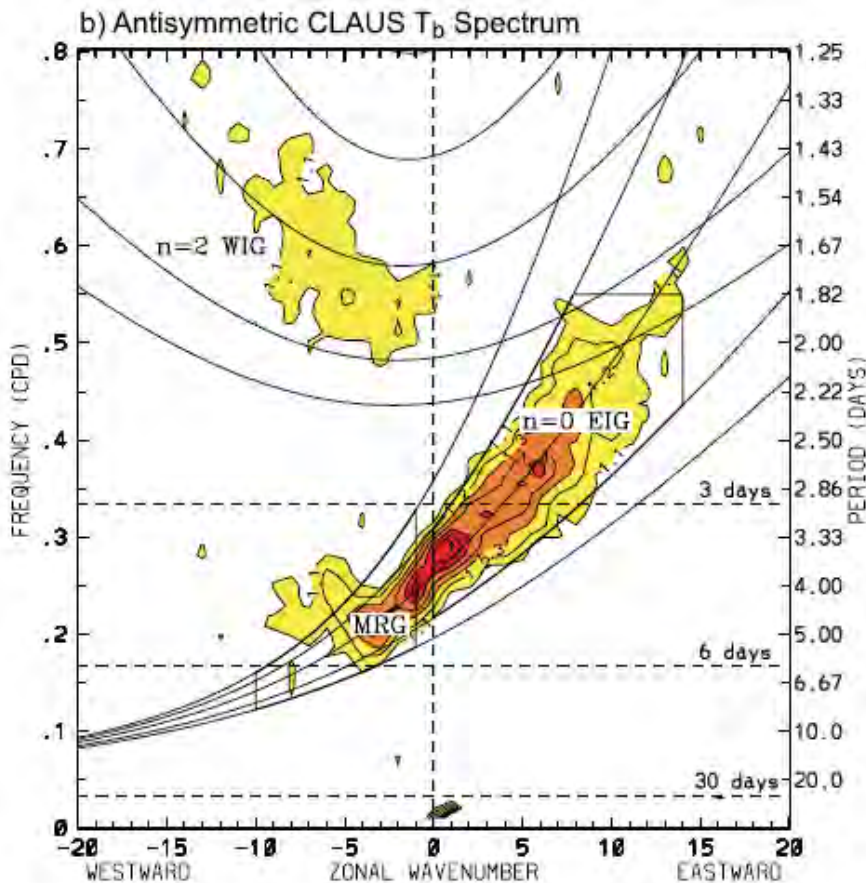
Main Topics:

- Coupling of equatorial wave to diabatic heating
- Equivalent depth
- Vertical structures of waves

In nature, atmospheric waves are **convectively coupled**. This means that the dry, shallow-water dynamics are coupled to diabatic heating (both latent *and* radiative heating).

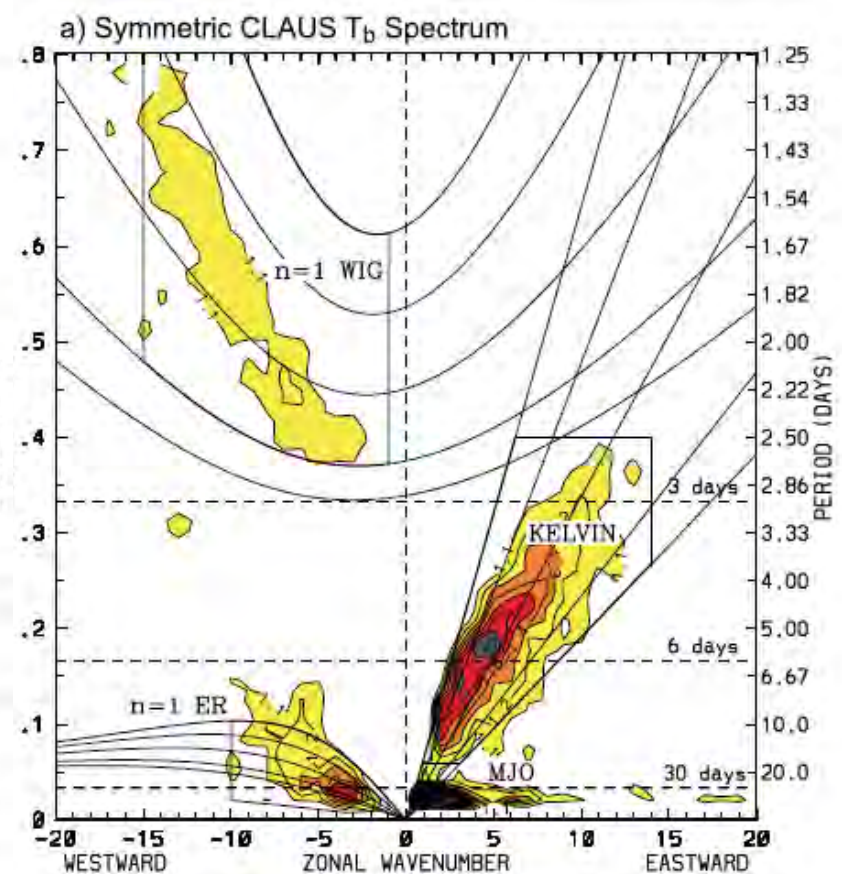
Convectively coupled waves move slower than their dry counterparts.

Asymmetric



Symmetric

Kiladis et al. (2009)



Rossby radius of deformation

$$R_e = \left(\frac{\sqrt{gh_e}}{\beta} \right)$$

depends on "equivalent depth"

$$h_e = \left(\frac{N^2}{g\lambda} \right)$$

This is not a physical depth in nature, but rather a depth of a shallow water wave that would give the phase speed observed in the real atmosphere.

TABLE 1. Vertical Structure Values for Dry Waves in a Constant N Atmosphere^a

h_e	L_z (km)	$\sqrt{gh_e}$ (m s ⁻¹)	R_e (Degrees Latitude)
<i>H = 7.3 km, dT₀/dz = -7.0 K km⁻¹ (Troposphere)</i>			
10	6.0	9.9	6.0
20	8.5	14.0	7.1
50	13.4	22.1	9.0
100	19.2	31.3	10.7
→ 200	27.9	44.3	12.7
500	47.5	70.0	15.9
<i>H = 6.1 km, dT₀/dz = +2.5 K km⁻¹ (Lower Stratosphere)</i>			
10	2.6	9.9	6.0
20	3.7	14.0	7.1
50	5.8	22.1	9.0
100	8.3	31.3	10.7
200	11.8	44.3	12.7
500	18.9	70.0	15.9

^aAs calculated from equation (17).

Rewrite state equations and add thermodynamic equation.

$$\begin{aligned}\frac{\partial u'}{\partial t} - \beta y v' + \frac{\partial \phi'}{\partial x} &= 0 \\ \frac{\partial v'}{\partial t} + \beta y u' + \frac{\partial \phi'}{\partial y} &= 0 \\ \frac{\partial \phi'}{\partial t} + c^2 \left(\frac{\partial u'}{\partial x} + \frac{\partial v'}{\partial y} \right) &= 0\end{aligned}$$

Let N be constant.

$$\begin{aligned}\frac{\partial u'}{\partial t} - \beta y v' + \frac{\partial \phi'}{\partial x} &= 0 \\ \frac{\partial v'}{\partial t} + \beta y u' + \frac{\partial \phi'}{\partial y} &= 0 \\ \frac{1}{\rho_0} \frac{\partial \rho_0 w'}{\partial z} + \left(\frac{\partial u'}{\partial x} + \frac{\partial v'}{\partial y} \right) &= 0 \\ \frac{\partial}{\partial t} \frac{\partial \phi'}{\partial z} + w N^2 &= 0\end{aligned}$$

Combine

$$\frac{\partial \phi'}{\partial t} + \frac{N^2}{\lambda} \left(\frac{\partial u'}{\partial x} + \frac{\partial v'}{\partial y} \right) = 0$$

$$\frac{\partial \phi'}{\partial t} + g h_e \left(\frac{\partial u'}{\partial x} + \frac{\partial v'}{\partial y} \right) = 0$$

For convectively coupled waves, diabatic heating is non-zero; therefore,

$$\frac{\partial}{\partial t} \frac{\partial \phi'}{\partial z} + wN^2 = Q$$

or in a form seen earlier in class...

$$\frac{\partial T'}{\partial t} - S\omega = Q$$

There are two ways to estimate the phase speed of coupled waves:

1) Determine the “effective static stability”, which depends on the offset between adiabatic and diabatic heating in the wave (if they completely cancel, then the wave is stationary in an atmosphere at rest.) The phase speed becomes

$$c_m = \sqrt{\left(1 + \frac{Q}{S\omega}\right) gh_e}$$

2) Explain propagation as the phase speed of higher baroclinic modes.

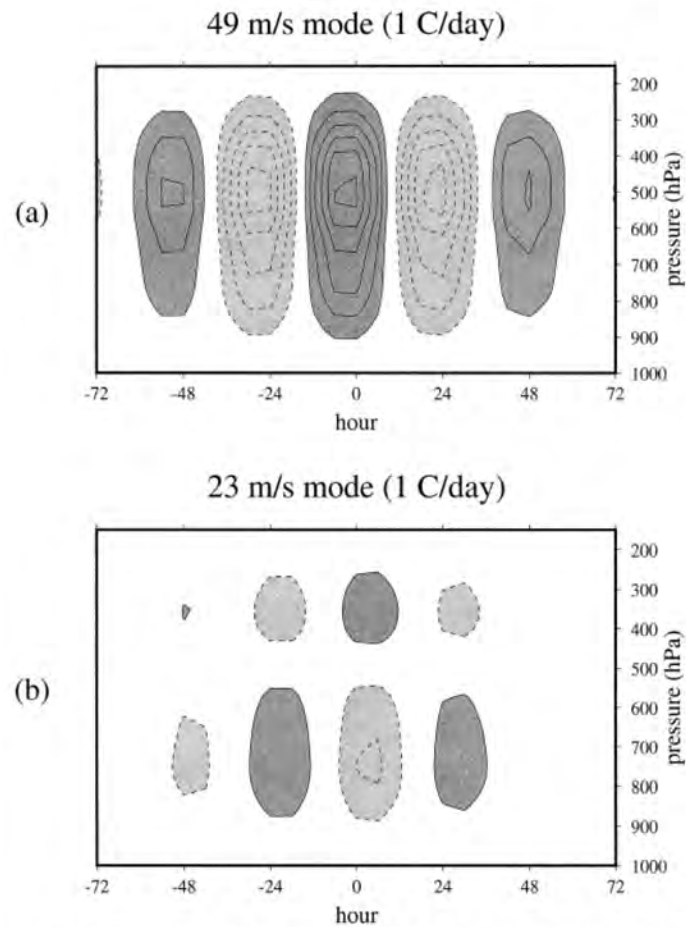


FIG. 8. A vertical mode decomposition of the observed perturbation heating for (a) the 49 m s^{-1} mode and (b) the 23 m s^{-1} mode. Each plot is shaded and contoured following the convection described in Fig. 4.

Haertel and Kiladis (2004)

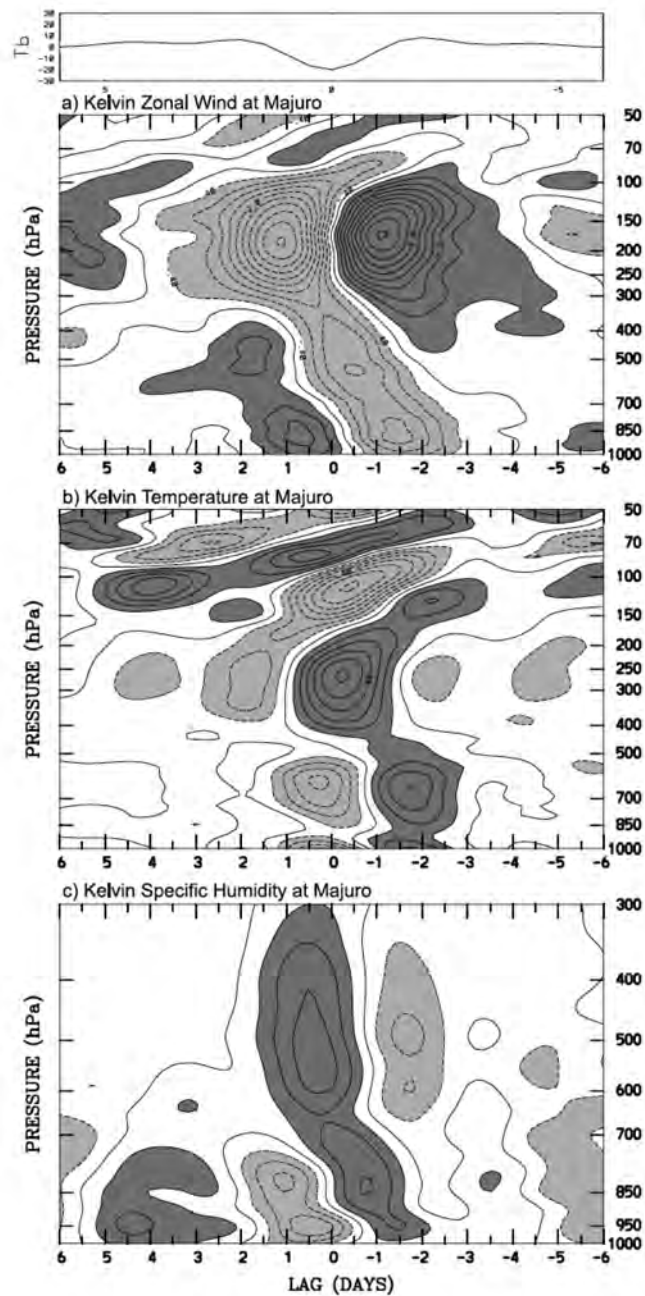
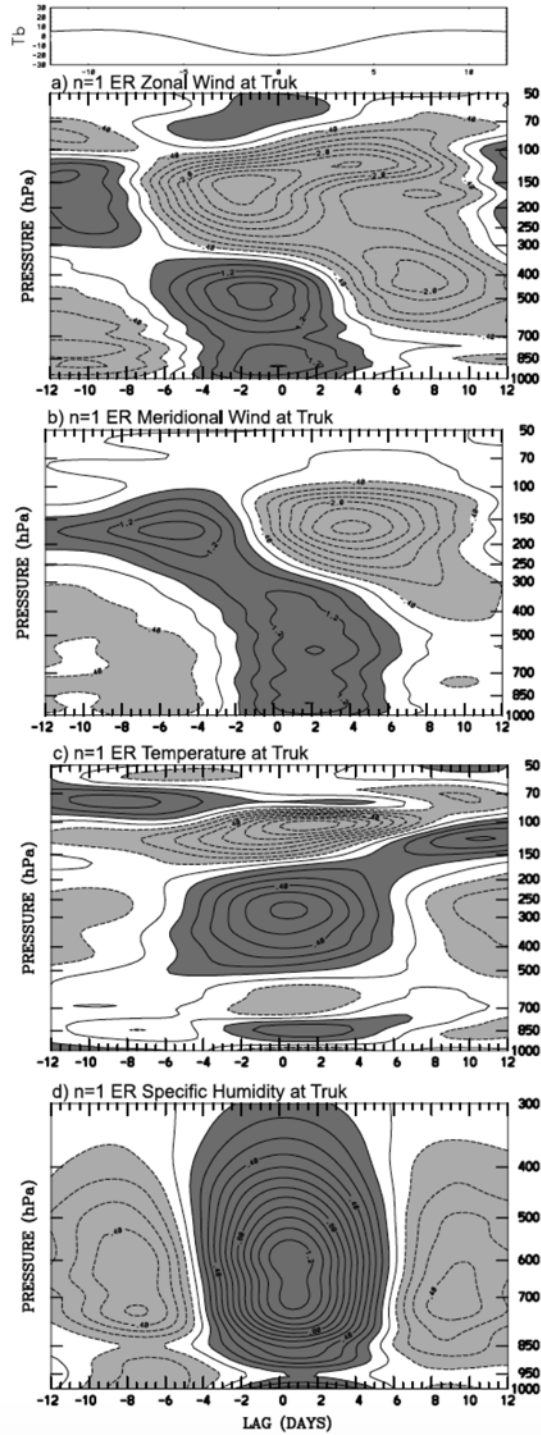


Figure 8. Time-height sections of anomalies of (a) zonal wind, (b) temperature, and (c) specific humidity at Majuro (7.1°N , 171.4°E), scaled to a -20 K perturbation in Kelvin filtered T_b at the nearest grid point on day 0. Contour interval is 0.4 m s^{-1} for wind, 0.1 K for temperature, and 0.1 g kg^{-1} for specific humidity, with negative contours dashed. Dark shading represents positive perturbations. The associated T_b anomaly is shown at the top in $^{\circ}\text{K}$.



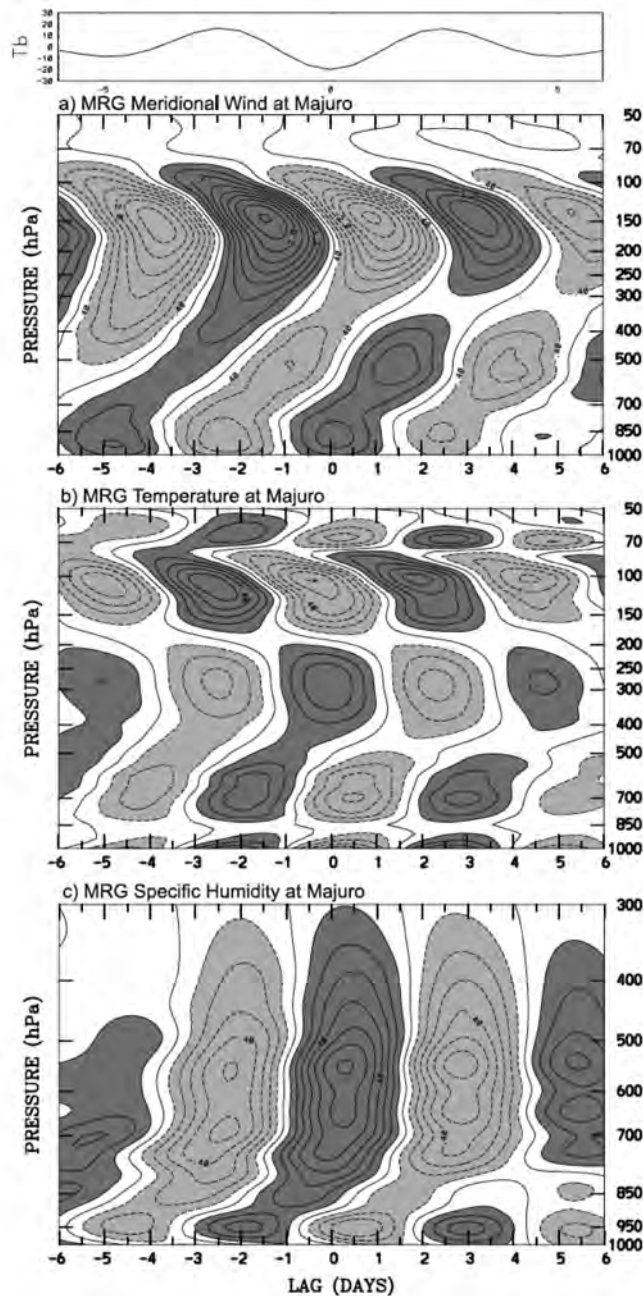


Figure 14. Time-height sections of anomalies in (a) meridional wind, (b) temperature, and (c) specific humidity at Majuro (7.1°N , 171.4°E), scaled to a -20 K perturbation in MRG filtered T_b at the nearest grid point on day 0. Contour interval is 0.4 m s^{-1} for wind, 0.1 K for temperature, and 0.1 g kg^{-1} for specific humidity, with negative contours dashed. Dark shading represents positive perturbations. The associated T_b anomaly is shown at the top in $^{\circ}\text{K}$.

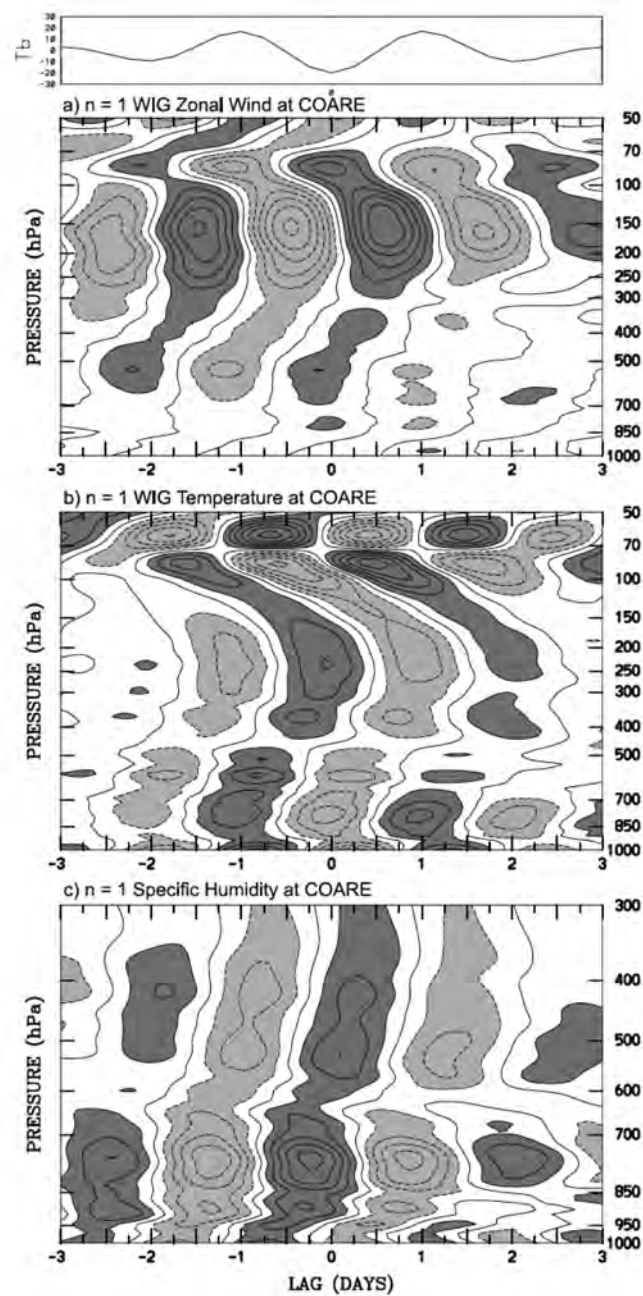
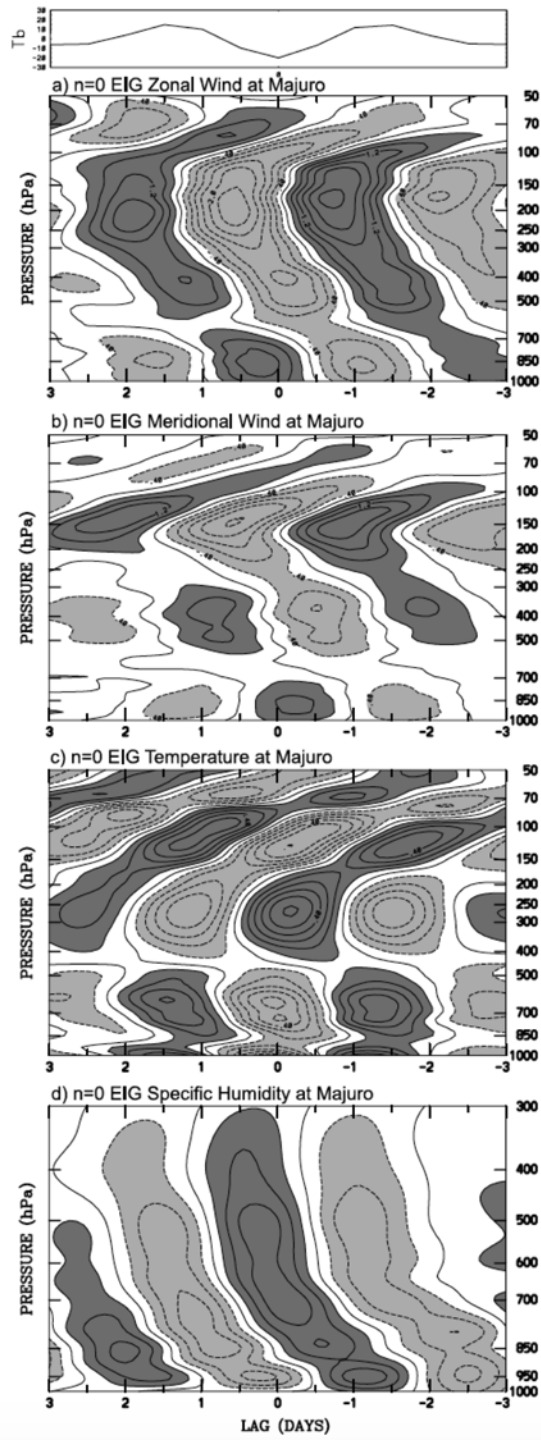


Figure 10. Time-height sections of anomalies of (a) zonal wind, (b) temperature, and (c) specific humidity within the COARE region centered on 2.0°S , 155.0°E , scaled to a -20 K perturbation in $n = 1$ WIG filtered T_b at the nearest grid point on day 0. Contour interval is 0.4 m s^{-1} for wind, 0.1 K for temperature, and 0.1 g kg^{-1} for specific humidity, with negative contours dashed. Dark shading represents positive perturbations. The associated T_b anomaly is shown at the top in $^{\circ}\text{K}$.



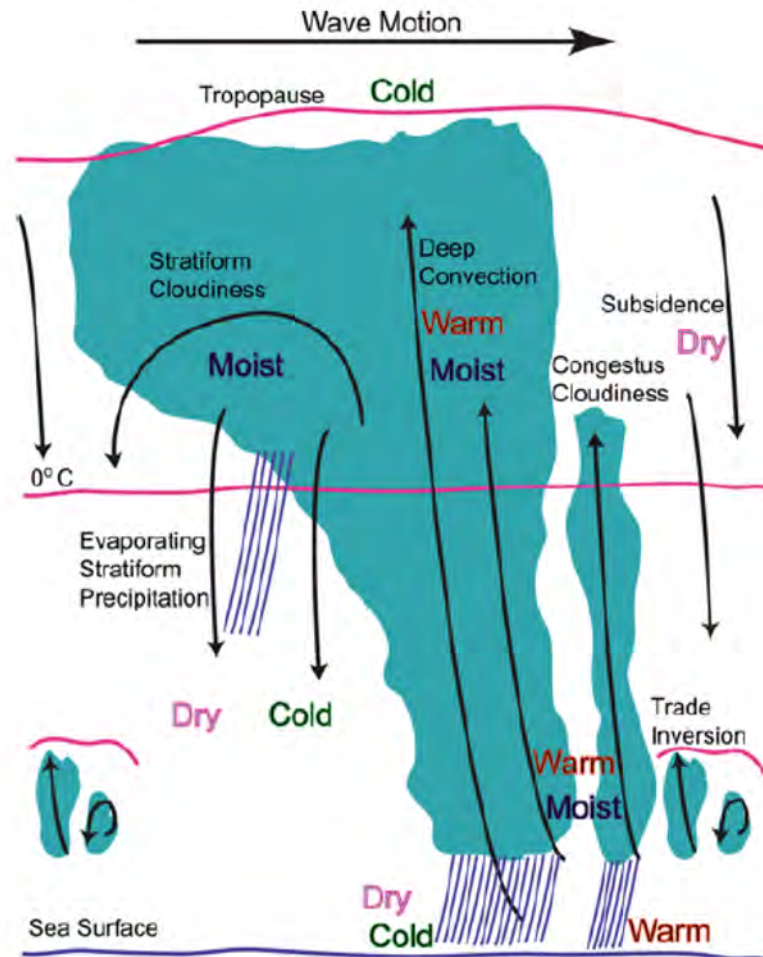


Figure 19. The hierarchy of cloudiness, temperature, and humidity within CCEWs, valid from MCS to MJO scales. Wave movement is from left to right (adapted from *Johnson et al.* [1999], *Straub and Kiladis* [2003c], and *Khouider and Majda* [2008]).

MR3252: Tropical Meteorology

Madden-Julian Oscillation (MJO)

Main Topics:

- MJO description
- Methods of identifying and tracking area of active MJO convection
- Velocity potential

What is the MJO?

Statistically significant 20–100 day variability in the timeseries of precipitation, surface pressure, zonal wind, and many other atmospheric variables at a location in the Tropics.

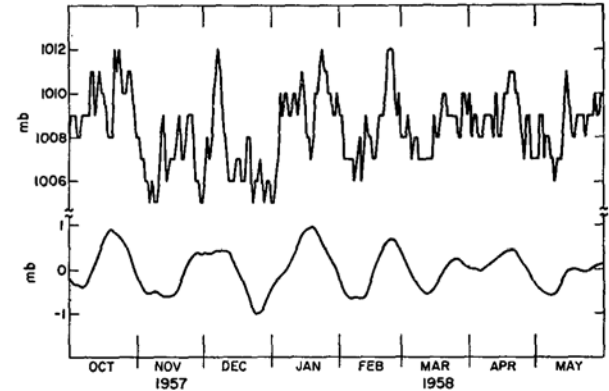


FIG. 9. Actual station pressures at Canton (top) and the corresponding pressures treated with a 45-day band-pass filter (bottom).

Madden and Julian (1972)

Strong MJO

Weak MJO

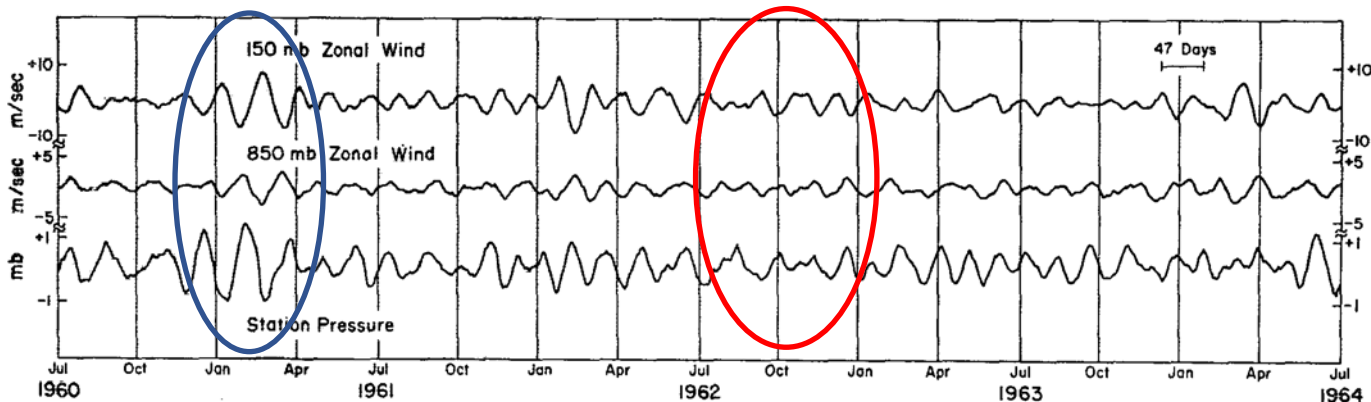
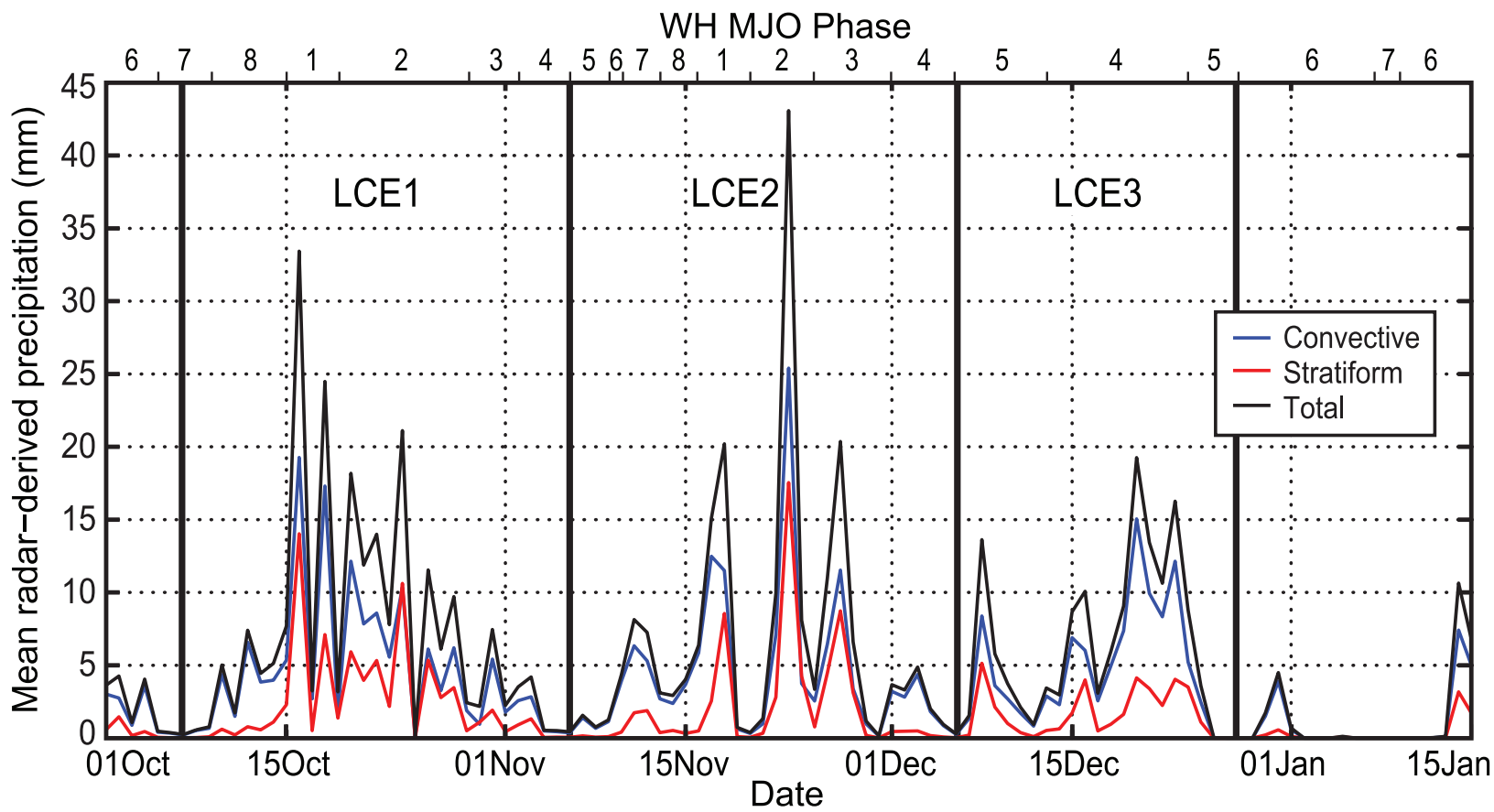


FIG. 5. The 150- and 850-mb u component and station pressure records for Canton Island from July 1960 through June 1964 treated with a 47-day band-pass filter.

Madden and Julian (1971)



Powell and Houze (2013)

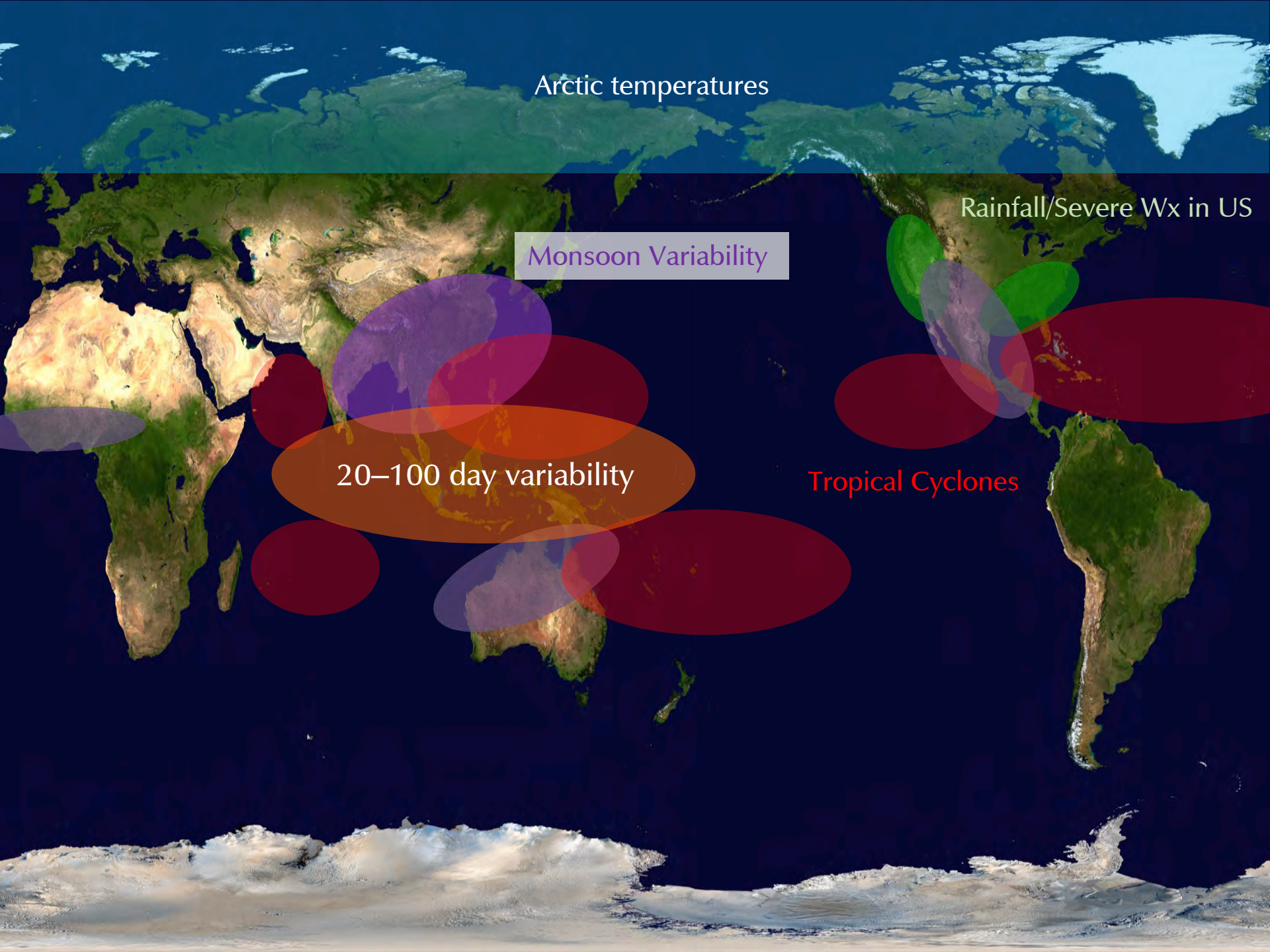
Arctic temperatures

Rainfall/Severe Wx in US

Monsoon Variability

20–100 day variability

Tropical Cyclones



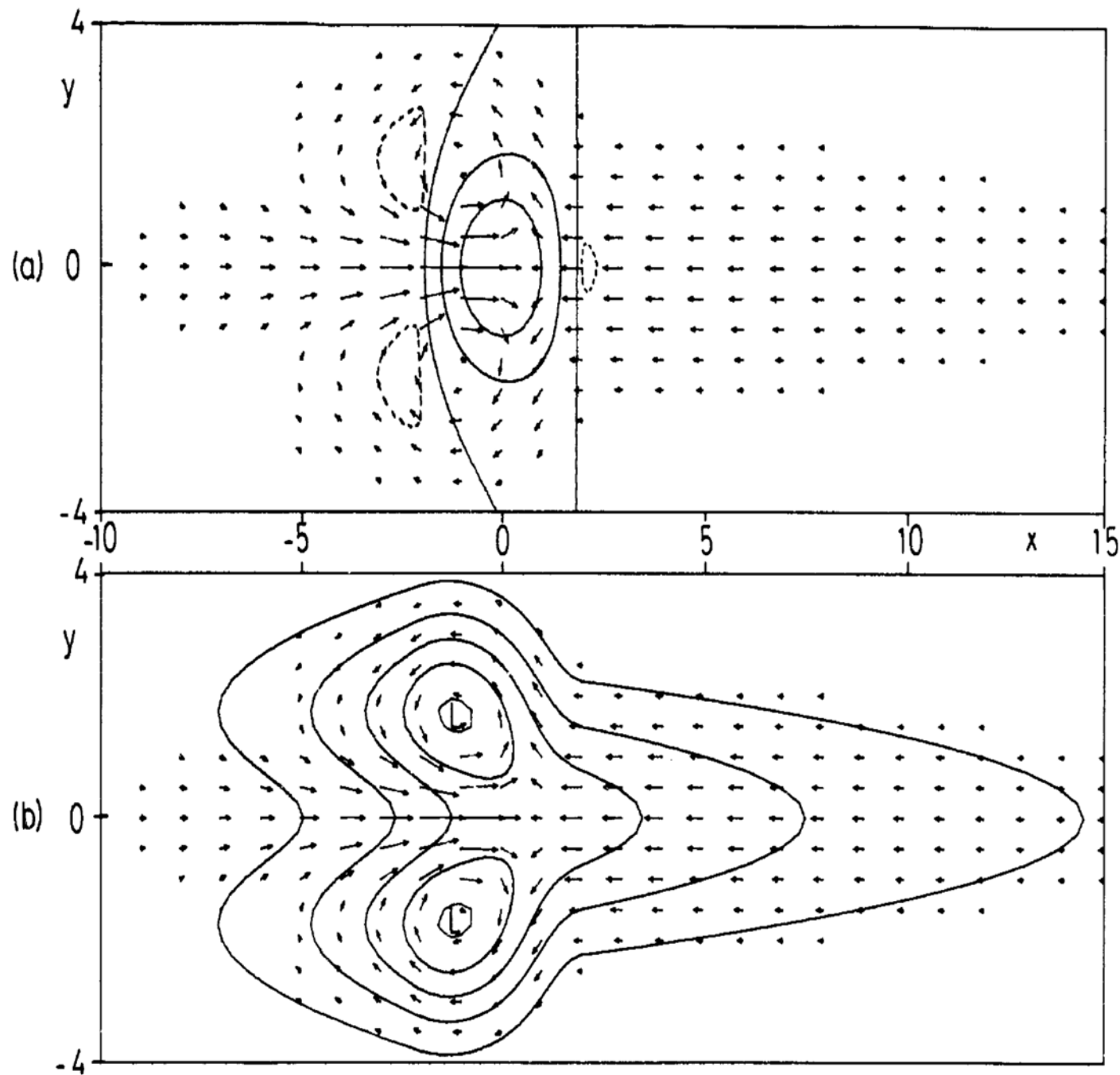
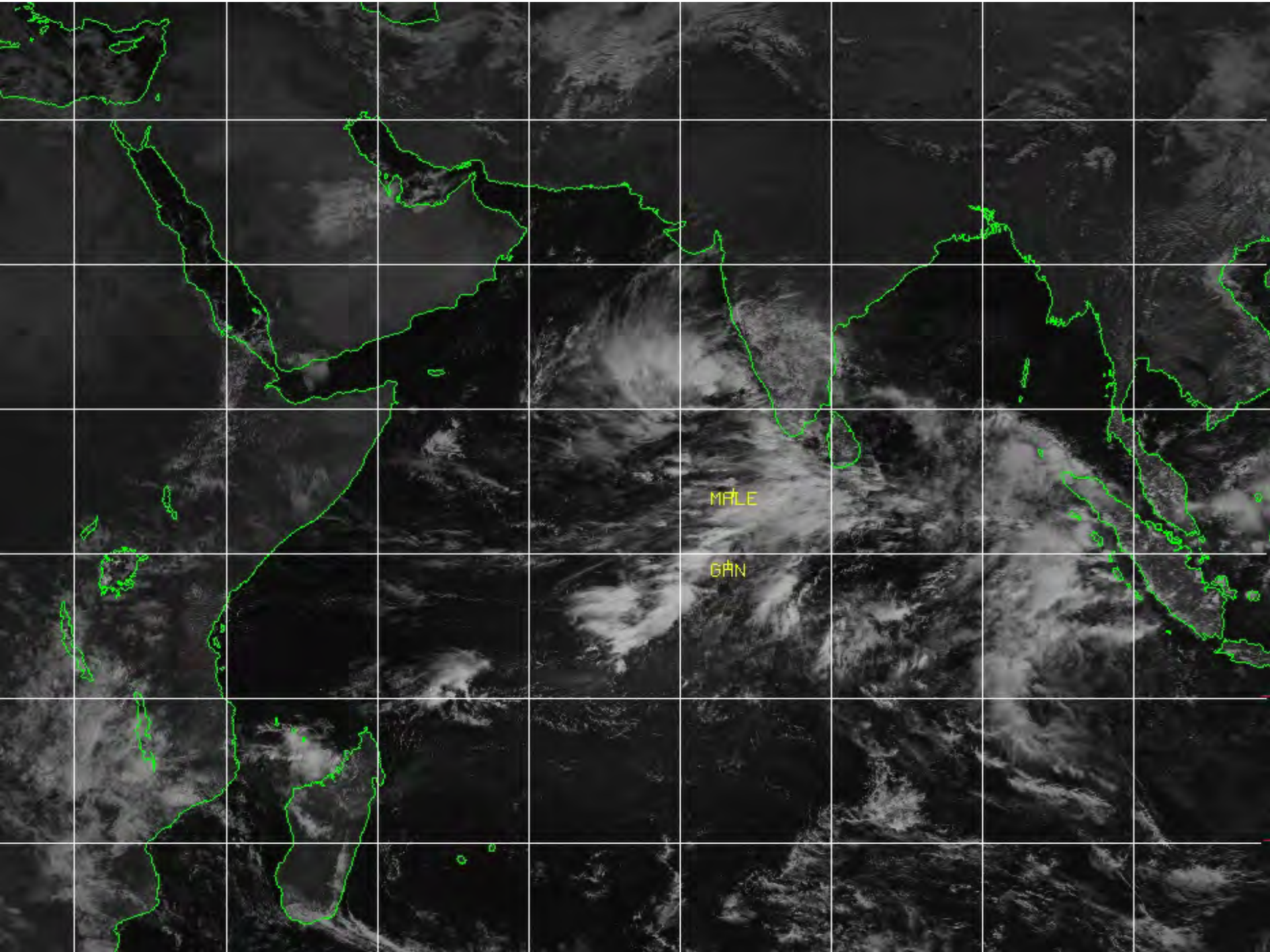


Figure 1. Solution for heating symmetric about the equator in the region $|x| < 2$ for decay factor $\varepsilon = 0.1$.

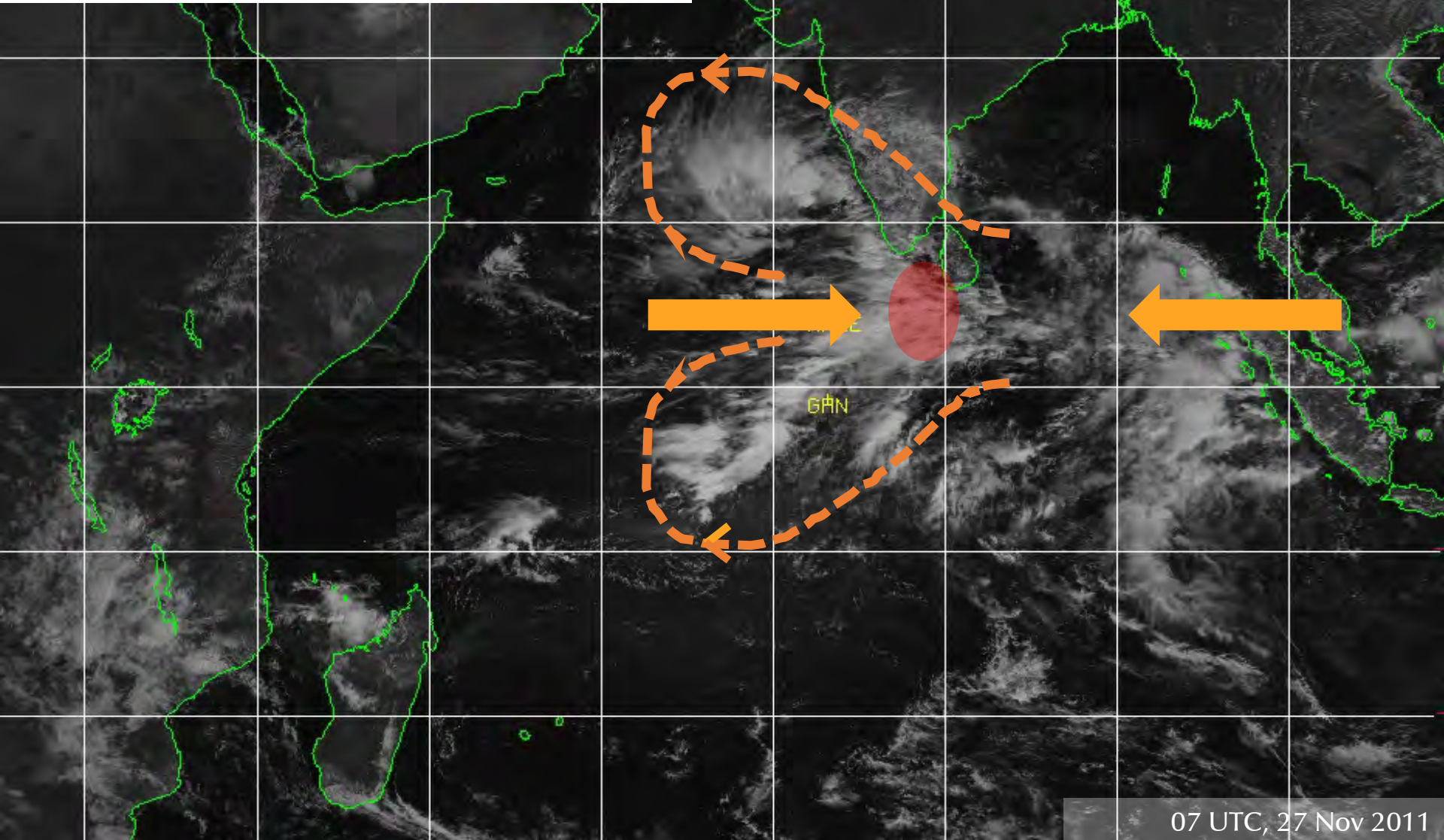
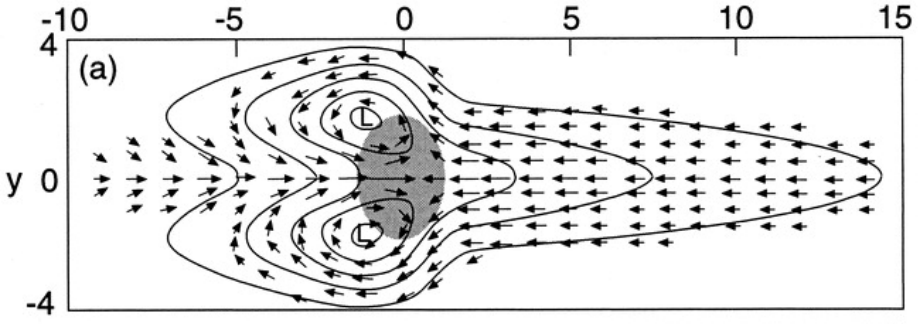
(a) Contours of vertical velocity w (solid contours are 0, 0.3, 0.6, broken contour is -0.1) superimposed on the velocity field for the lower layer. The field is dominated by the upward motion in the heating region where it has approximately the same shape as the heating function. Elsewhere there is subsidence with the same pattern as the pressure field.

(b) Contours of perturbation pressure p (contour interval 0.3) which is everywhere negative. There is a trough at the equator in the easterly régime to the east of the forcing region. On the other hand, the pressure in the westerlies to the west of the forcing region, though depressed, is high relative to its value off the equator. Two cyclones are found on the north-west and south-west flanks of the forcing region.



MPL

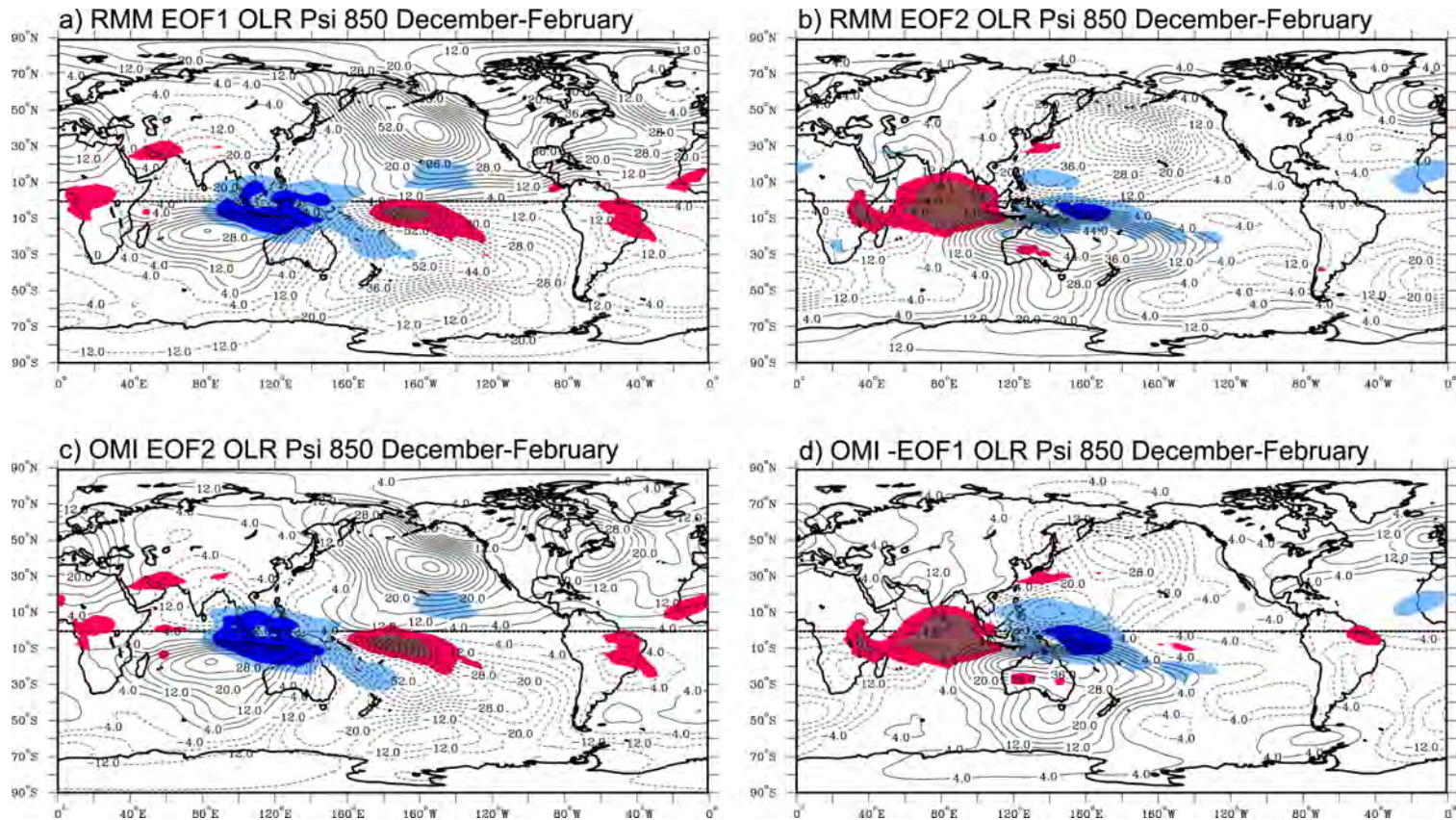
GAN



07 UTC, 27 Nov 2011

Objective Identification of MJO

Several indices are used to identify the MJO objectively in real-time. None are perfect, and each emphasizes a different atmospheric variable (such as OLR, zonal wind, velocity potential) or weights those variables differently.



First two EOFs explain about 25% of variance in RMM.

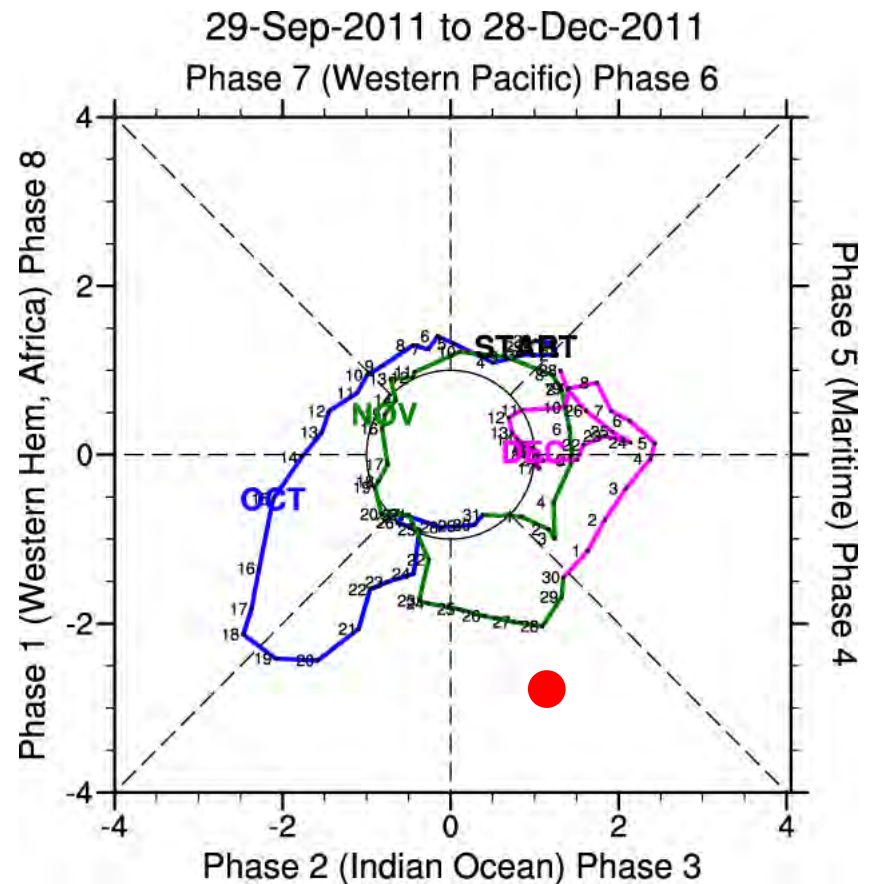
MJO indices are usually split into “phases” that indicate how OLR and/or zonal wind project onto the first two EOFs of their variability.

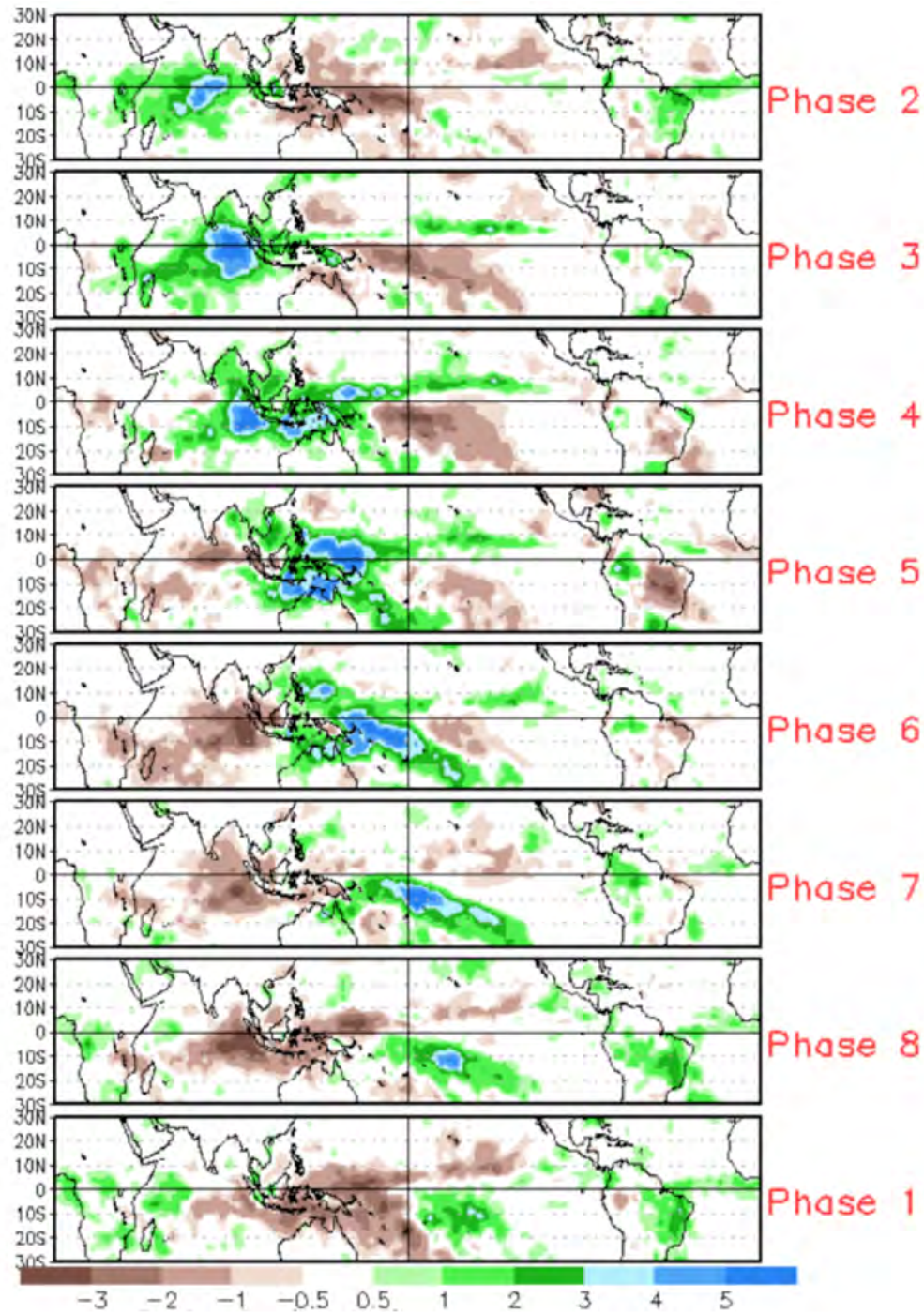
- Phase 1: $|PC1| > |PC2|$, $PC1, PC2 < 0$
- Phase 2: $|PC1| < |PC2|$, $PC1, PC2 < 0$
- Phase 3: $|PC1| < |PC2|$, $PC1 > 0, PC2 < 0$
- Phase 4: $|PC1| > |PC2|$, $PC1 > 0, PC2 < 0$
- Phase 5: $|PC1| > |PC2|$, $PC1, PC2 > 0$
- Phase 6: $|PC1| < |PC2|$, $PC1, PC2 > 0$
- Phase 7: $|PC1| < |PC2|$, $PC1 < 0, PC2 > 0$
- Phase 8: $|PC1| > |PC2|$, $PC1 < 0, PC2 > 0$

Usually, $\sqrt{PC1^2 + PC2^2} > 1$ is a requirement for a signal to be considered a statistically robust MJO.

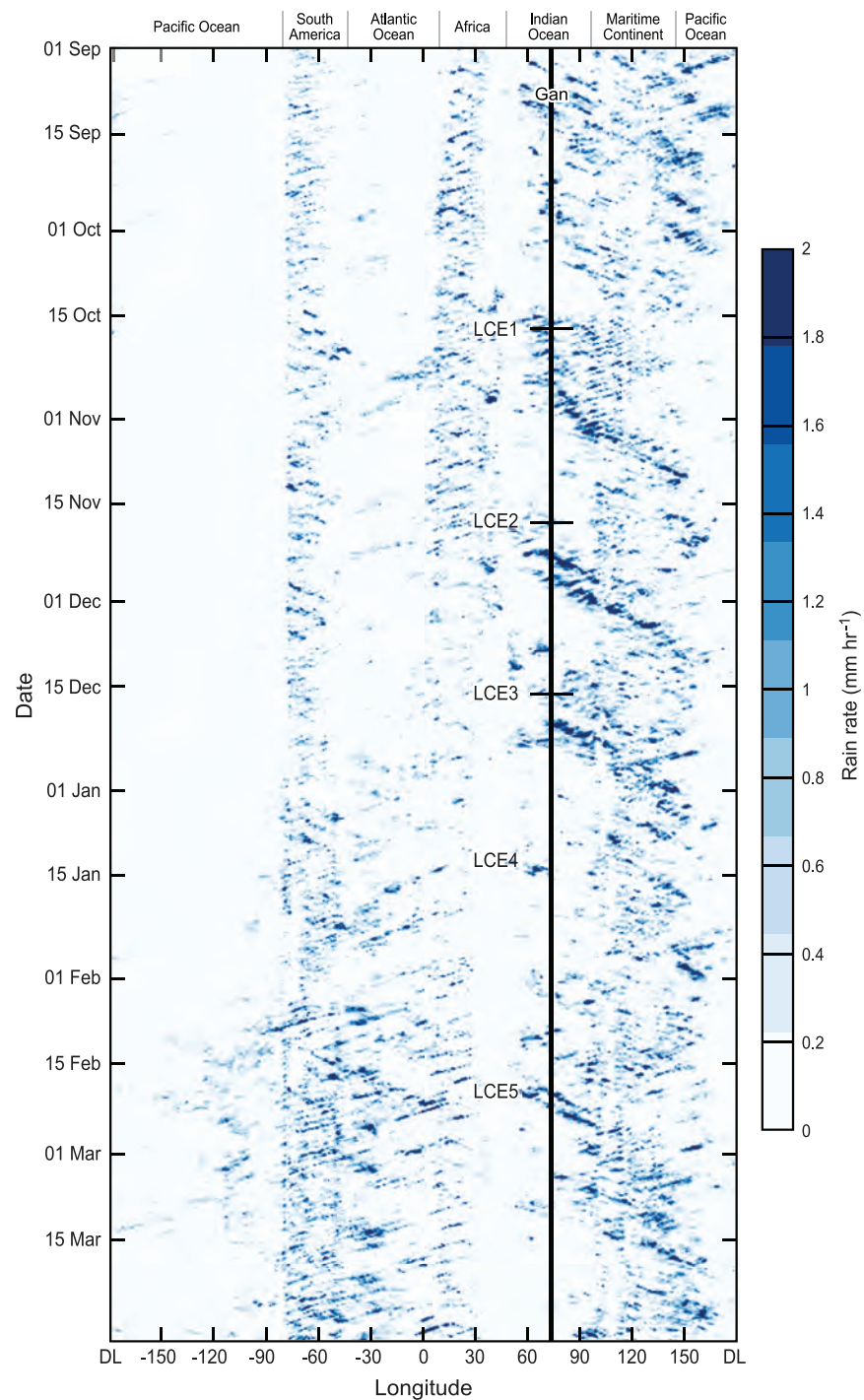
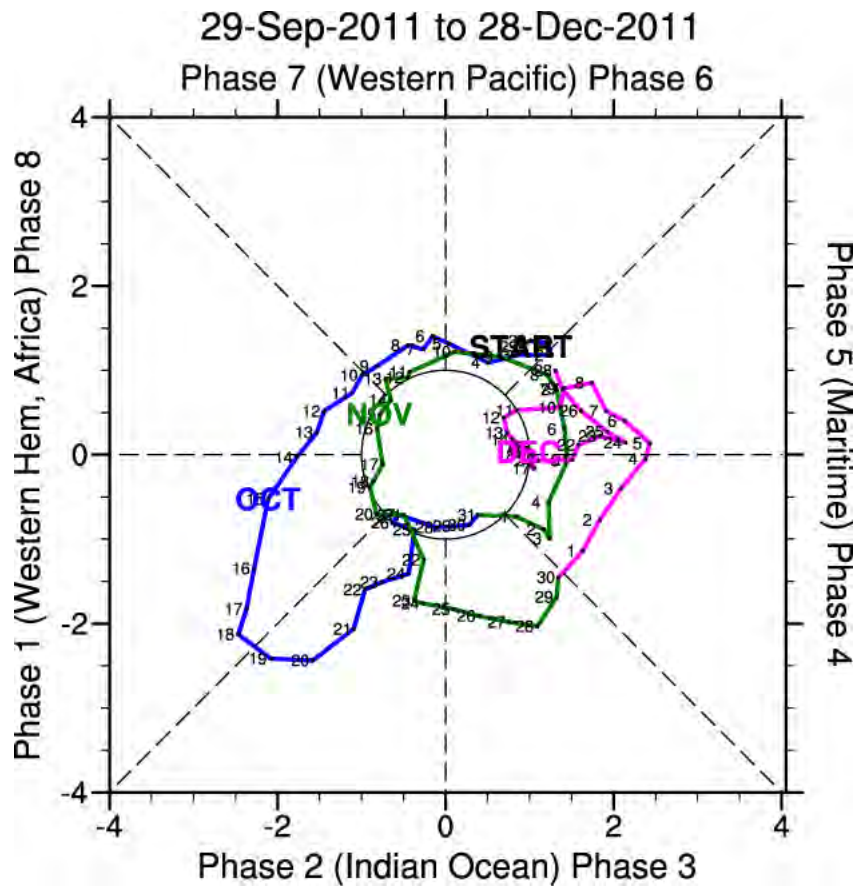
Old examples of RMM (BoM):

<http://www.bom.gov.au/climate/mjo/>





NOAA



Some other indices

Index	Description	Obtain timeseries
OMI The OLR MJO Index	Projection of 20-96 day filtered OLR, including all eastward and westward wave numbers onto the daily spatial EOF patterns of 30-96 day eastward filtered OLR.	OMI values UPDATED
OOMI The Original OLR MJO Index	Projection of 30-96 day eastward only filtered OLR onto the spatial EOF patterns of 30-96 day eastward filtered OLR. This results in a smoother index than OMI due to more restrictive filtering.	OOMI values
ROMI The Real-time OLR MJO Index	Projection of 9 day running average OLR anomalies onto the daily spatial EOF patterns of 30-96 day eastward filtered OLR. OLR anomalies are calculated by first subtracting the previous 40 day mean OLR. The running average is tapered as the target date is approached.	ROMI values
FMO The Filtered OLR MJO index.	Univariate EOF of normalized 20-96 day filtered OLR averaged from 15S-15N, by longitude. The same spatial EOF pattern is used for the entire year (see below).	FMO values
VPM The Velocity Potential MJO index.	Calculated in the same way as the Wheeler-Hendon RMM, except using 200 hPa Velocity Potential instead of OLR, along with U200 and U850 in a combined EOF (see link to Ventrice et al. 2013 below).	VPM values

Some other indices

OMI: Only uses OLR to determine EOFs

VPM: Uses velocity potential wind zonal wind to determine EOFs.

What is velocity potential? An assessment of the irrotational component of the large-scale flow.

We can break up the vector wind (\mathbf{u}) into rotational and divergent components.

Irrotational means $\nabla \times \mathbf{u}_d = \mathbf{0}$ $\mathbf{u}_d = \nabla \cdot \mathbf{u}$

Nondivergent means $\nabla \cdot \mathbf{u}_r = \mathbf{0}$ $\mathbf{u}_r = \nabla \times \mathbf{u}$

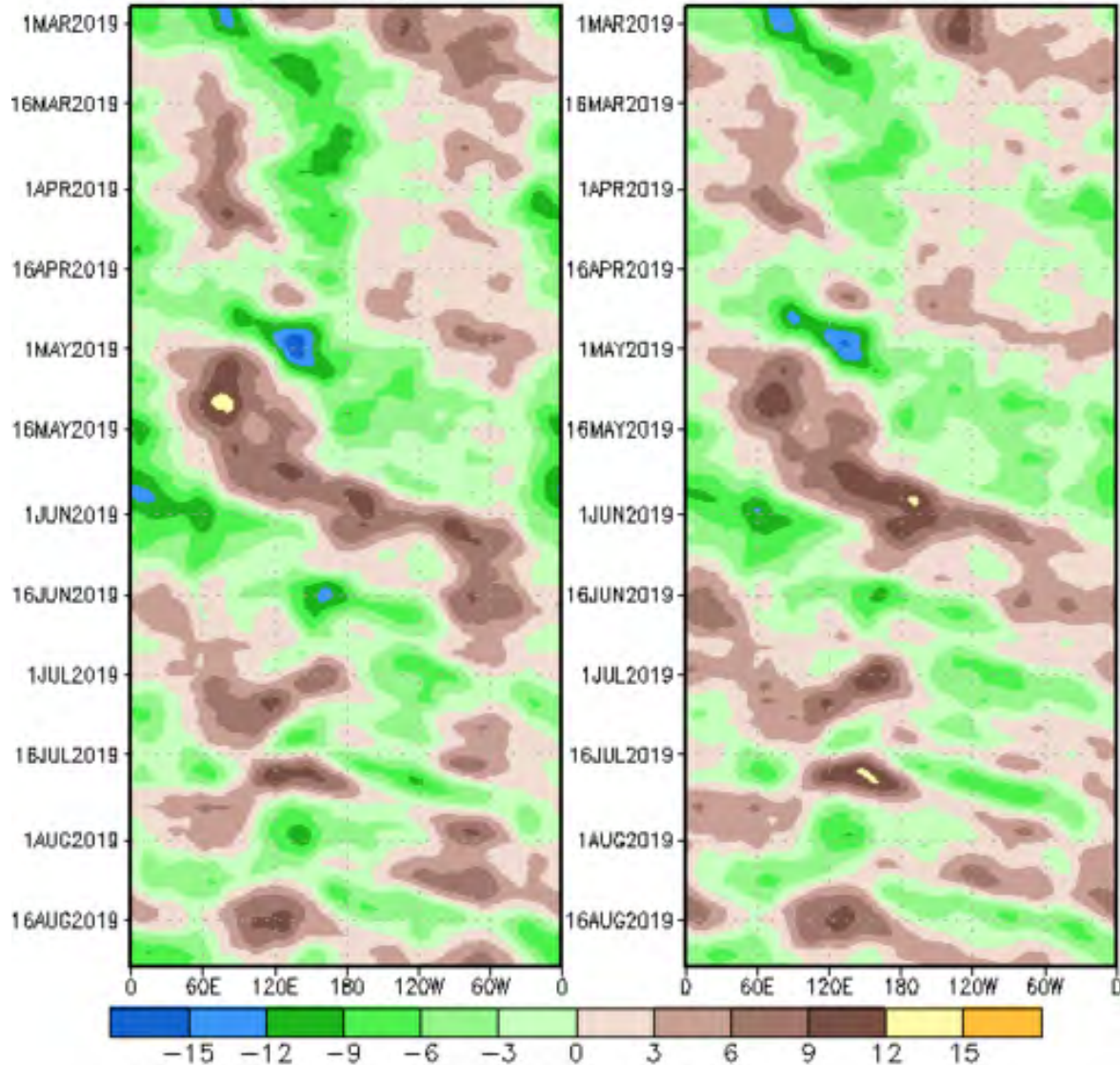
The velocity potential (χ) is defined as $\mathbf{u}_d = \nabla \chi \longrightarrow \chi = \nabla^{-1} \mathbf{u}_d$

A negative velocity potential represents large-scale divergent flow.

200-hPa Velocity Potential Anomaly: 5N–5S

5-day Running Mean

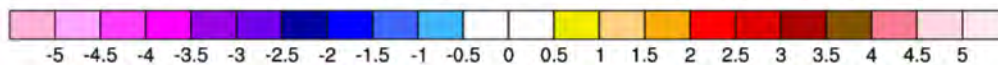
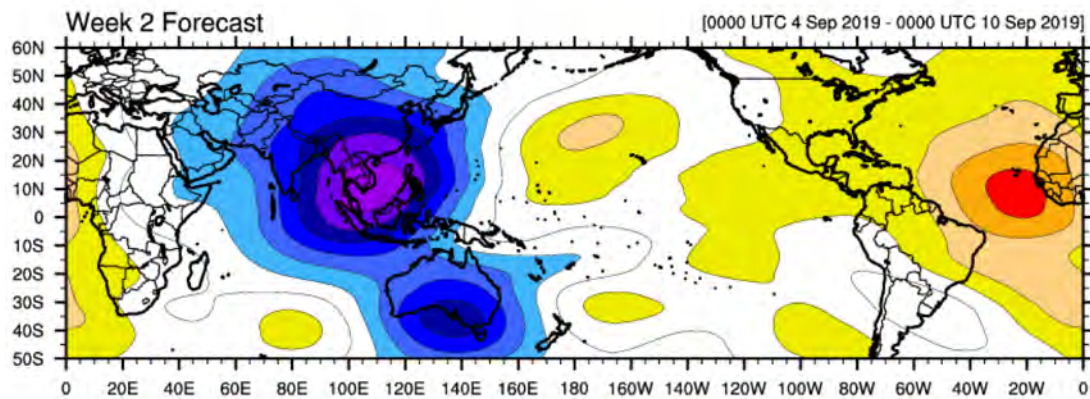
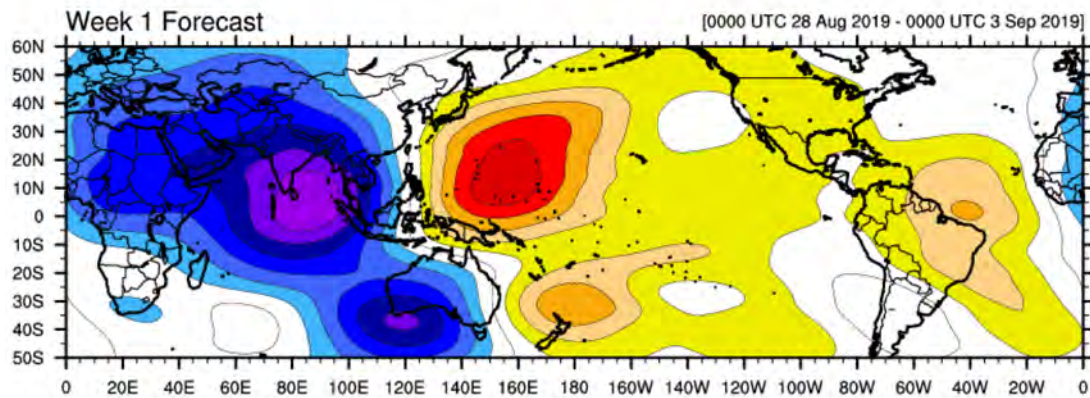
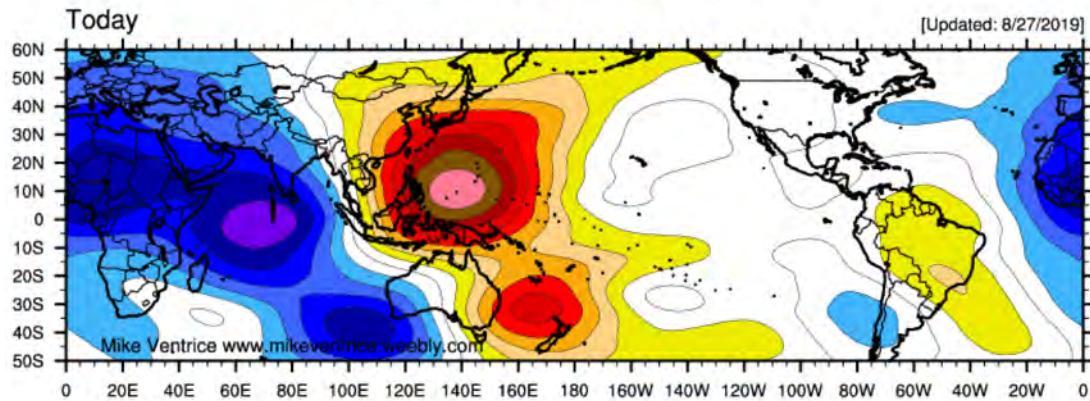
Period-Mean Removed



Data updated through 25 AUG 2019

NOAA/CPC

MJO filtered VP200 Forecast



Mike Ventrice

MR3252: Tropical Meteorology

MJO Dynamics

Main Topics:

- Initialization of MJO Convection
- Maintenance of MJO
- Overview of MJO theories

Fundamental Features of the MJO

- Low-frequency, high wavenumber; Dominated by variability with wavenumber 1 or 2
- Eastward propagation of convection with a mean of 5 m/s, but varying between events
- Moves faster when not strongly coupled to convection
- Irregular 30–90 day period
- Sometimes clearly connected to prior MJO event; however, some MJO events appear to occur with no obvious precursor

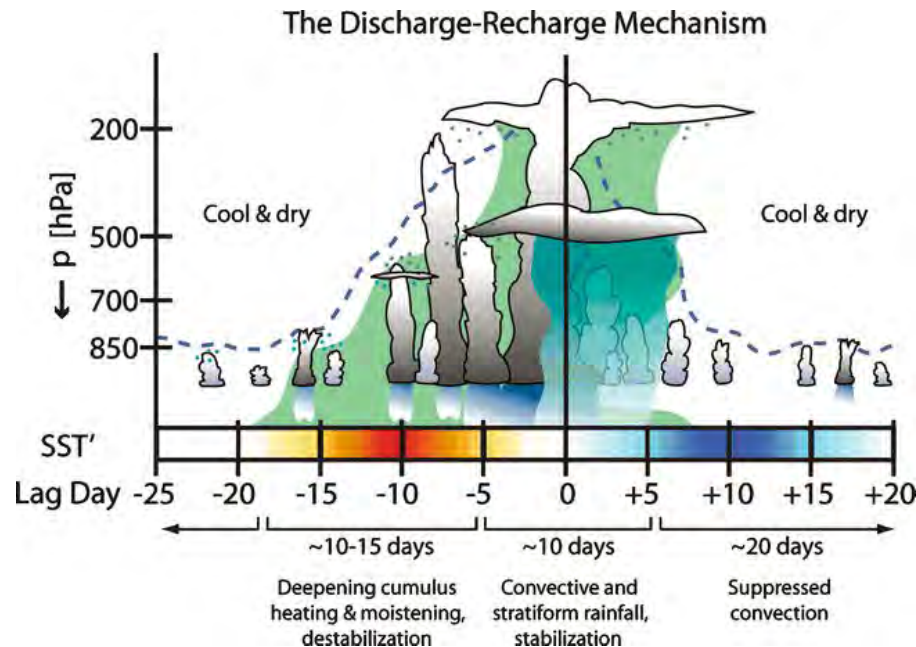
What causes an episode of MJO convection to first develop?

This has long been thought of as a “chicken and egg” problem:

- Convection causes moistening of the troposphere, and yet
- Deep convection needs ample moisture in the troposphere to overcome entrainment

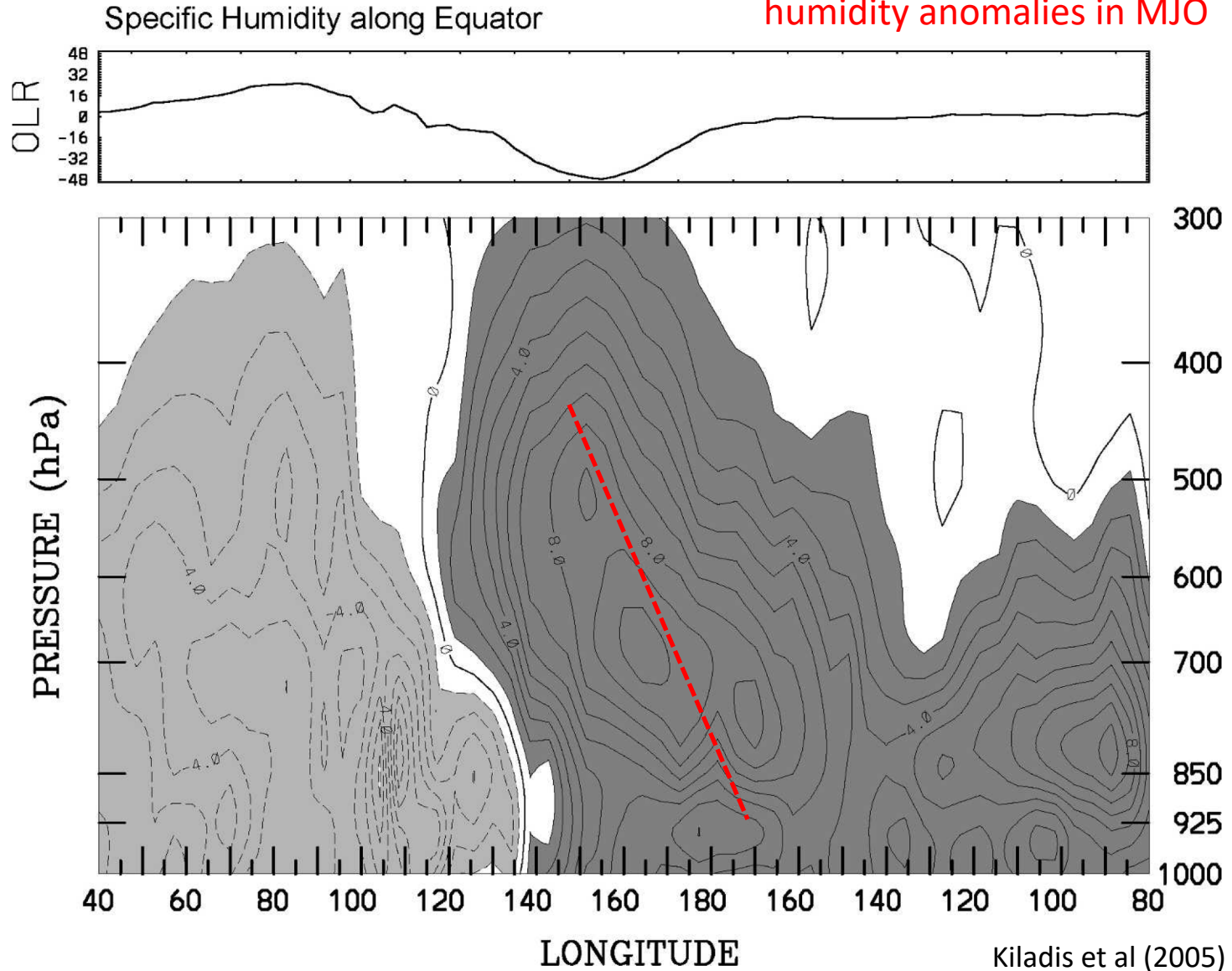
There are other ways to moisten the environment, mainly horizontal advection of moist air.

So which does come first, the convection or the moisture? This is a question about whether clouds are actively involved in moistening the atmosphere or passively respond to changes in the large-scale environment.



Benedict and Randall
(2007)

Tilted structure of specific humidity anomalies in MJO



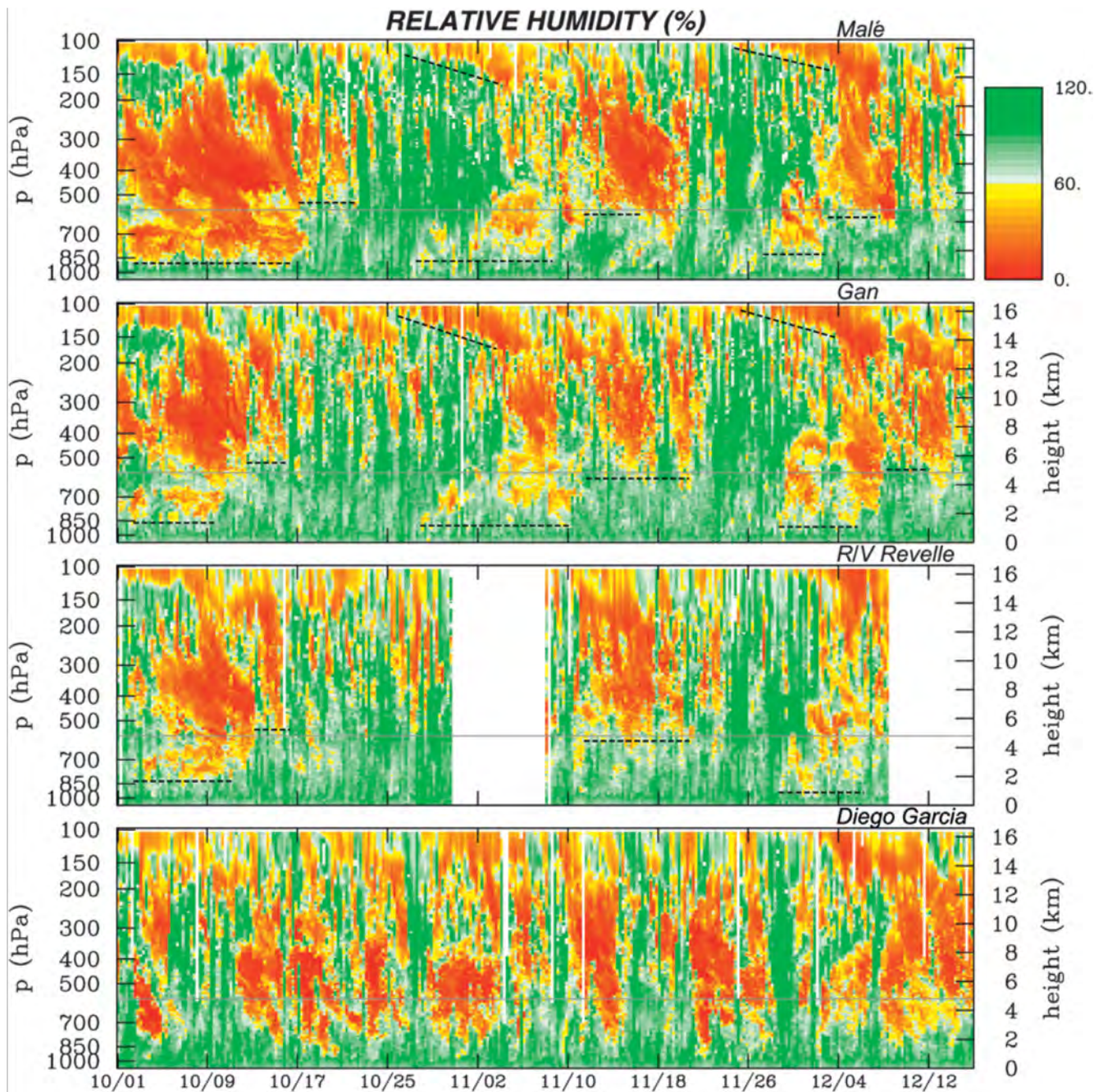


FIG. 13. Time series of relative humidity (%; with respect to ice for $T < 0^{\circ}\text{C}$) from 1 Oct to 15 Dec at Malé, Gan Island, R/V Revelle, and Diego Garcia based on full time resolution of sounding data. See Fig. 1 for site locations. Dotted line segments denote approximate tops of moist layers. Thin gray line denotes 0°C level.

Table 3. Maximum Lagged Cross-Correlation Coefficients (With Lag in Hours in Parentheses) Between Convective/Stratiform Areal Coverage and Unfiltered, Unsmoothed Specific Humidity Anomalies for 1 October to 15 January Using Various Smoothing Periods^a

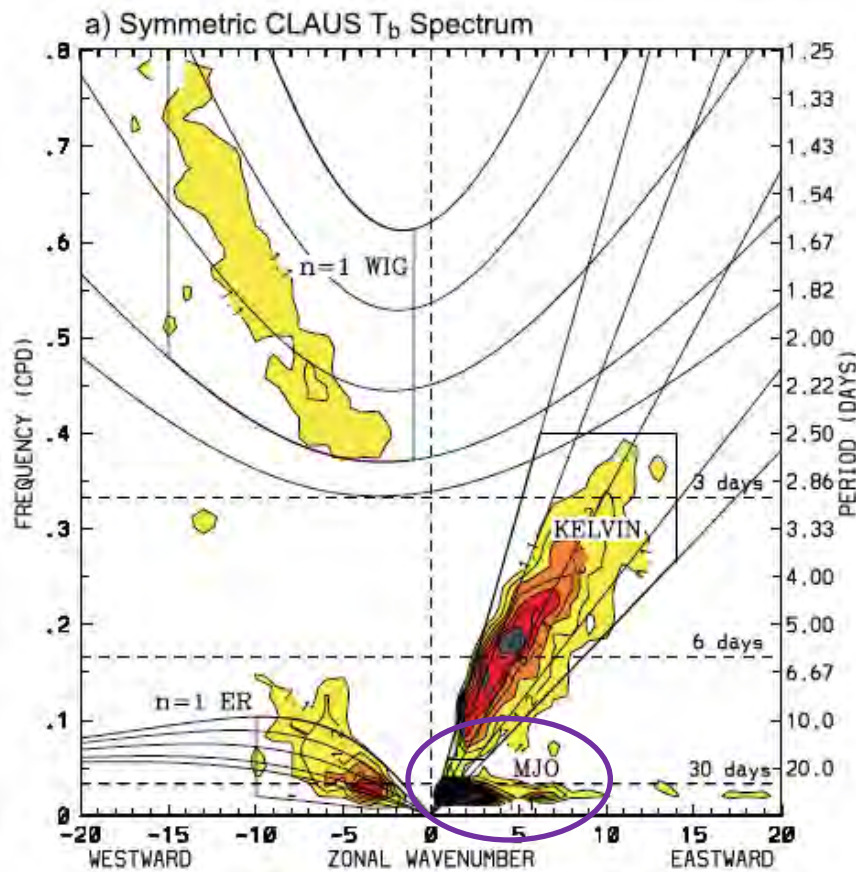
Var. 1	Var. 2	Smoothing Interval					
		None	6h	12h	24h	36h	72h
Conv	q'_{850}	0.45 (0)	0.49 (0)	0.54 (0)	0.60 (0)	0.61 (0)	0.69 (0)
Conv	q'_{700}	0.50 (+3)	0.53 (0)	0.58 (0)	0.66 (0)	0.70 (0)	0.80 (0)
Conv	q'_{500}	0.49 (+6)	0.51 (+6)	0.54 (+12)	0.61 (+24)	0.61 (+36)	0.73 (+72)
Conv	q'_{300}	0.44 (+9)	0.47 (+6)	0.51 (+12)	0.50 (0)	0.51 (+36)	0.59 (+72)
Strat	q'_{850}	0.34 (-3)	0.37 (-6)	0.39 (-12)	0.42 (-24)	0.46 (-36)	0.54 (-72)
Strat	q'_{700}	0.45 (-3)	0.47 (0)	0.50 (0)	0.55 (0)	0.61 (0)	0.77 (0)
Strat	q'_{500}	0.55 (+3)	0.57 (0)	0.60 (0)	0.65 (0)	0.70 (0)	0.76 (0)
Strat	q'_{300}	0.52 (+3)	0.56 (0)	0.61 (0)	0.66 (0)	0.68 (0)	0.74 (0)
Conv	Strat	0.81 (+3)	0.80 (+6)	0.76 (0)	0.80 (0)	0.82 (0)	0.81 (0)

^aAll correlation values that are in bold are statistically significant at the 95% level. Variables correlated are shown in columns 1 and 2. Positive lags indicate that Variable 1 comes first. (Conv=Convective areal coverage; Strat=Stratiform areal coverage).

Simple radar analysis strongly suggests that convection leads tropospheric moistening, and therefore probably plays an active role in “preconditioning” the atmosphere for deeper convection. *More on this in paper discussion.*

How does the MJO maintain itself and propagate eastward?

For this question, traditional shallow water theory is insufficient. None of the dispersion lines on the Wheeler and Kiladis power spectrum diagram match up with the OLR power in the MJO band.



If we include moisture feedbacks into the linear model of equatorial waves, we can produce “moisture modes”. Mathematically, this requires an assumption that temperature gradients in the free-troposphere are weak (i.e. weak temperature gradient, or WTG theory).

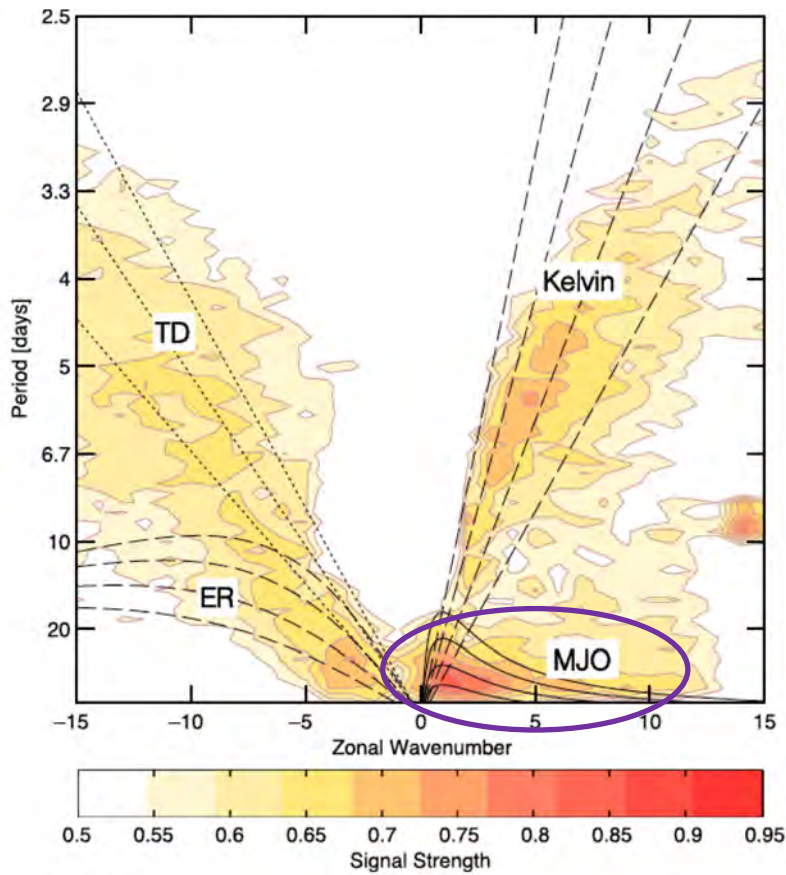


FIG. 13. Signal strength of symmetric OLR anomalies averaged over the 15°N–15°S latitude belt. The MJO-related dispersion curves (solid lines) correspond to frequencies obtained from Eq. (29a) for $L = 13\,200$ km, $\tau_c = 13.7$ h, and A_{KR} of 25, 40, 60, and $80 \times 10^{-9} \text{ m}^{-1}$. Dispersion curves are also plotted for Kelvin and ER (dashed lines) for h_e of 12, 25, 50, and 90 m. Dotted lines indicate constant phase speeds of 7.0, 9.0, and 11.0 m s^{-1} , which are representative of westward-propagating TD and easterly waves [see also Yasunaga and Mapes (2012)]. Contour interval is every 0.05 signal strength fraction beginning at 0.55.

Adames and Kim (2016)

$$\tilde{\omega} = -\frac{i}{\tau_c} \left[\frac{\sqrt{2}}{2} (\Gamma_{uK} + 2\Gamma'_{uR}) \delta q_u + \frac{\sqrt{2}}{4} n \Gamma'_{vR} \bar{q}_0 + \tilde{M}_{\text{eff}}^* \right], \quad (16)$$

where

Cloud-radiative feedback

$$\tilde{M}_{\text{eff}}^* = 1 - \frac{\sqrt{2} \bar{M}_{q0}}{2M_s} (1 + r) \quad (17)$$

is the projected effective gross moist stability. As noted by SM, this dispersion relation is complex and only the terms involving Γ_{uK} , Γ_{uR} , and Γ_{vR} , which arise from the horizontal wind field through Eq. (12) can be real and determine the propagation of the moist wave, while the other terms determine the growth and dissipation. Separating the dispersion relation into its real and imaginary parts yields the following:

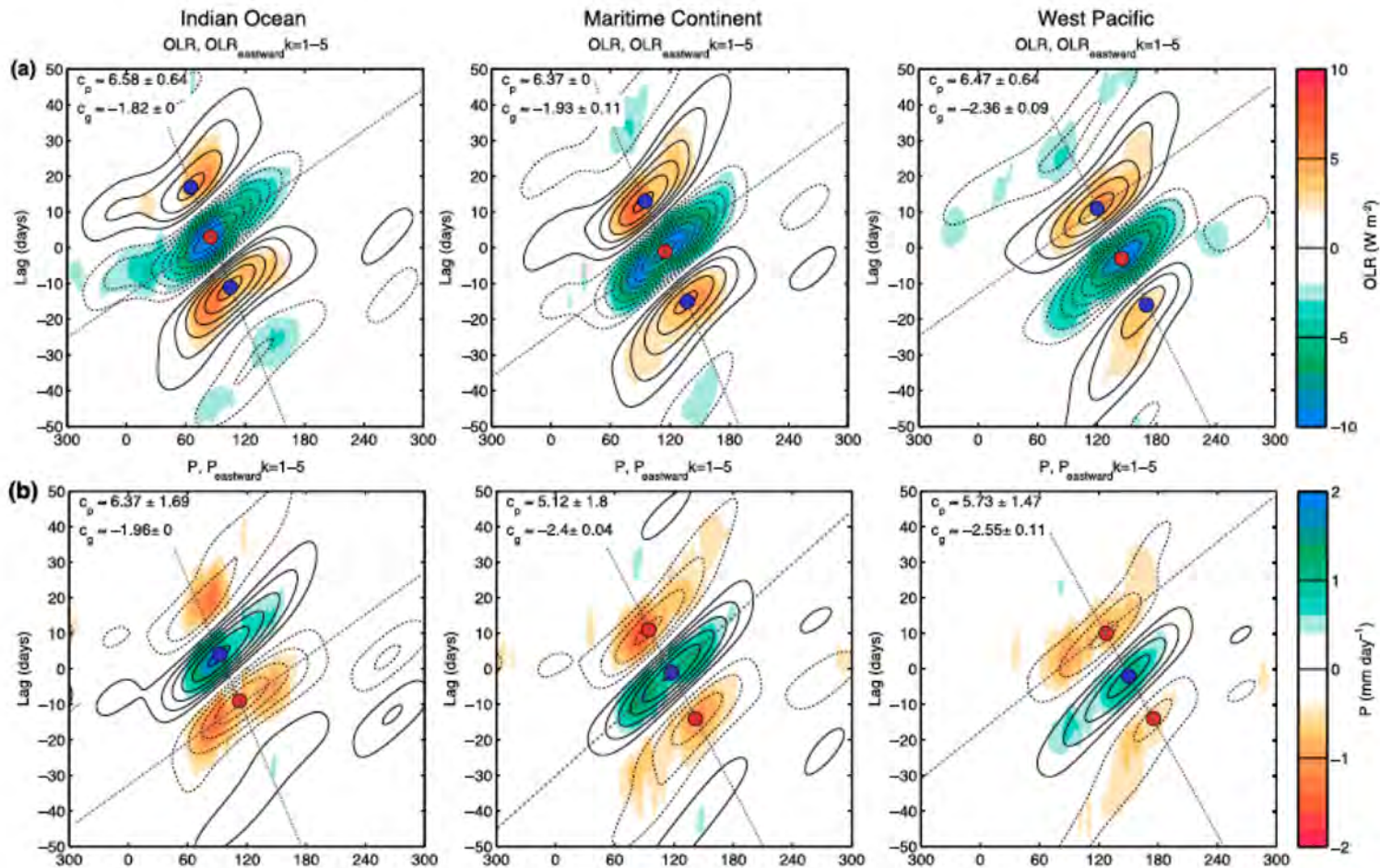
$$\text{Re}(\tilde{\omega}) = \frac{1}{\tau_c k} (\tilde{p}_K A_K + \tilde{p}_R A_R) \quad \text{and} \quad (18a)$$

$$\text{Im}(\tilde{\omega}) = -\frac{1}{\tau_c} \left(\frac{\tilde{p}_K A_K}{k \tan \alpha_K} + \frac{\tilde{p}_R A_R}{k \tan \alpha_R} + \tilde{M}_{\text{tot}}^* \right). \quad (18b)$$

The real component of the dispersion relation is solely due to the Kelvin and Rossby waves inducing moistening and drying by horizontal and vertical moisture advection and modulating the mean surface latent heat fluxes and high-frequency eddy activity. We define this induced moistening/drying as

$$A_K = \frac{\sqrt{2}}{2} \delta q_u \hat{V} (1 + r) \quad \text{and} \quad (19a)$$

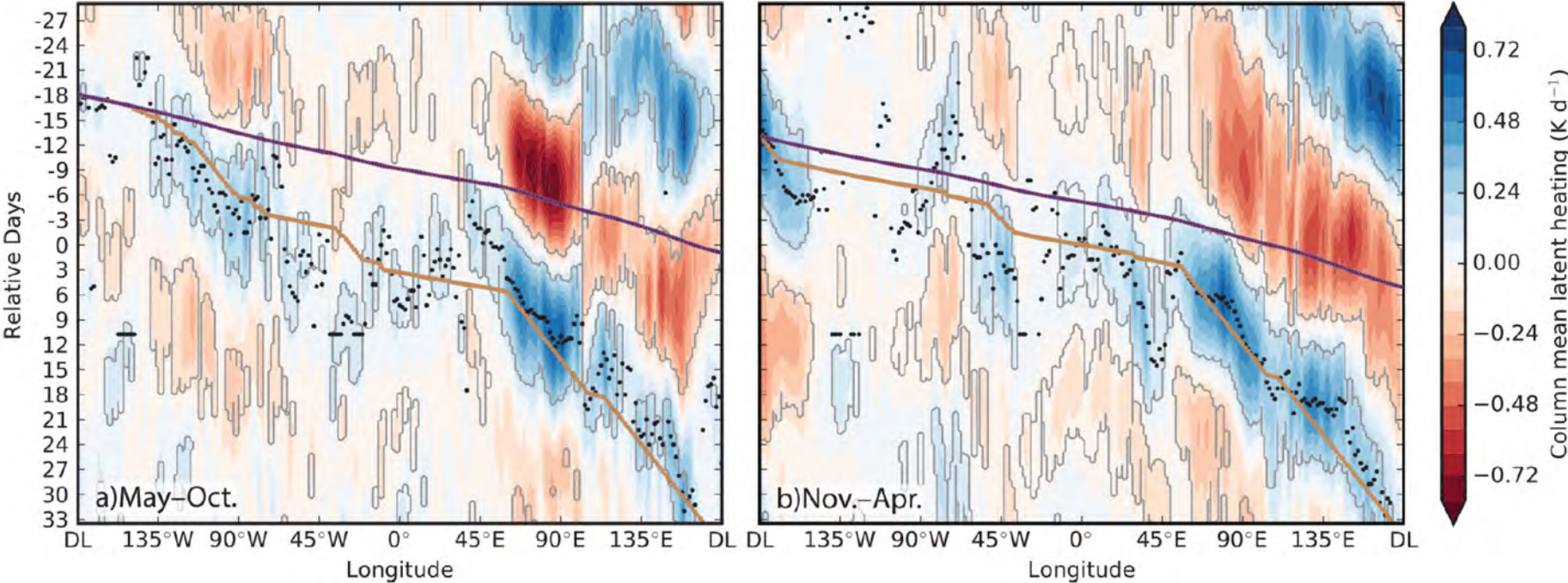
$$A_R = \sqrt{2} (\delta q_u + 2n \bar{q}_0 L^{-1}) \hat{V} (1 + r), \quad (19b)$$



Adames and Kim (2016)

The dispersion relation yields an eastward phase speed and westward group velocity, meaning the MJO is dispersive. Cloud radiative feedbacks favor growth of low-wavenumber modes.

Powell (2017)



MJO propagates like a moisture wave at times, but as convectively coupled Kelvin wave at other times, *even if diabatic heating anomaly is small.*

Other MJO theories

- Convection-dynamics-moisture trio-interaction theory: MJO is a convectively coupled Kelvin-Rossby with boundary layer convergence occurring ahead, or to the east of the convective heating.
 - Growth of MJO governed by feedback between clouds and radiation and between BL frictional convergence and diabatic heating
 - BL feedback causes eastward propagation
- Skeleton Model: MJO is an envelope of numerous synoptic-scale and mesoscale convection.
 - Wave activity growth with lower tropospheric moisture.
 - Eastward propagation caused by positive moisture anomalies to east of active convection
- Gravity wave theory: MJO is a region of synoptic-scale westward and eastward propagating inertio-gravity waves.
 - Does not require moisture
 - Eastward propagation explained by asymmetric between propagation of eastward and westward propagating inertio-gravity waves.